

# PLATINUM-GROUP ELEMENTS IN THE AFTON CU-AU PORPHYRY DEPOSIT, SOUTHERN BRITISH COLUMBIA

By Graham T. Nixon<sup>1</sup>

**KEYWORDS:** Cu-Au porphyry, alkaline, Iron Mask Batholith, platinum-group elements, copper-iron sulphides, geology, geochemistry, Afton, picrite

## INTRODUCTION

Alkaline intrusive complexes associated with Cu-Au porphyry deposits in British Columbia (Barr *et al.*, 1976) are currently the focus of investigations funded by the "Rocks to Riches" Program, B. C. and Yukon Chamber of Mines, to determine the potential of these magmatic-hydrothermal systems for platinum-group elements (PGE). Although there are reports of trace amounts of PGE, specifically palladium, in smelter concentrates from Cu-Au porphyry deposits in the province, very little is known about actual abundances in the mineralized rocks and ores being mined. To address this deficiency, data pertaining to PGE mineralization in alkaline complexes has recently been published by Nixon and Carbo (2001), Dunn *et al.* (2001), Nixon (2001, 2002, 2003) and Nixon and Peatfield (2003); and PGE occurrences pertaining to these and other geological environments in the province have been compiled by Hulbert (2001).

A new exploration initiative by DRC Resources Corporation at the Afton mine near Kamloops provided an opportunity to sample core carrying Cu-Au-Ag-PGE mineralization encountered during deep-drilling beneath and beyond the open pit. The core recovered and assayed by DRC Resources allowed a small suite of samples to be collected from PGE-enriched intervals for mineralogical study and multi-element analysis using different analytical techniques. This report presents quantitative data for the PGE and other metals in mineralized drill core from Afton, and petrographic observations of the host rocks, ore minerals and alteration assemblages. These new data, albeit from a small sample suite, allow for a preliminary assessment of the nature and origin of the PGE-bearing sulphide mineralization.

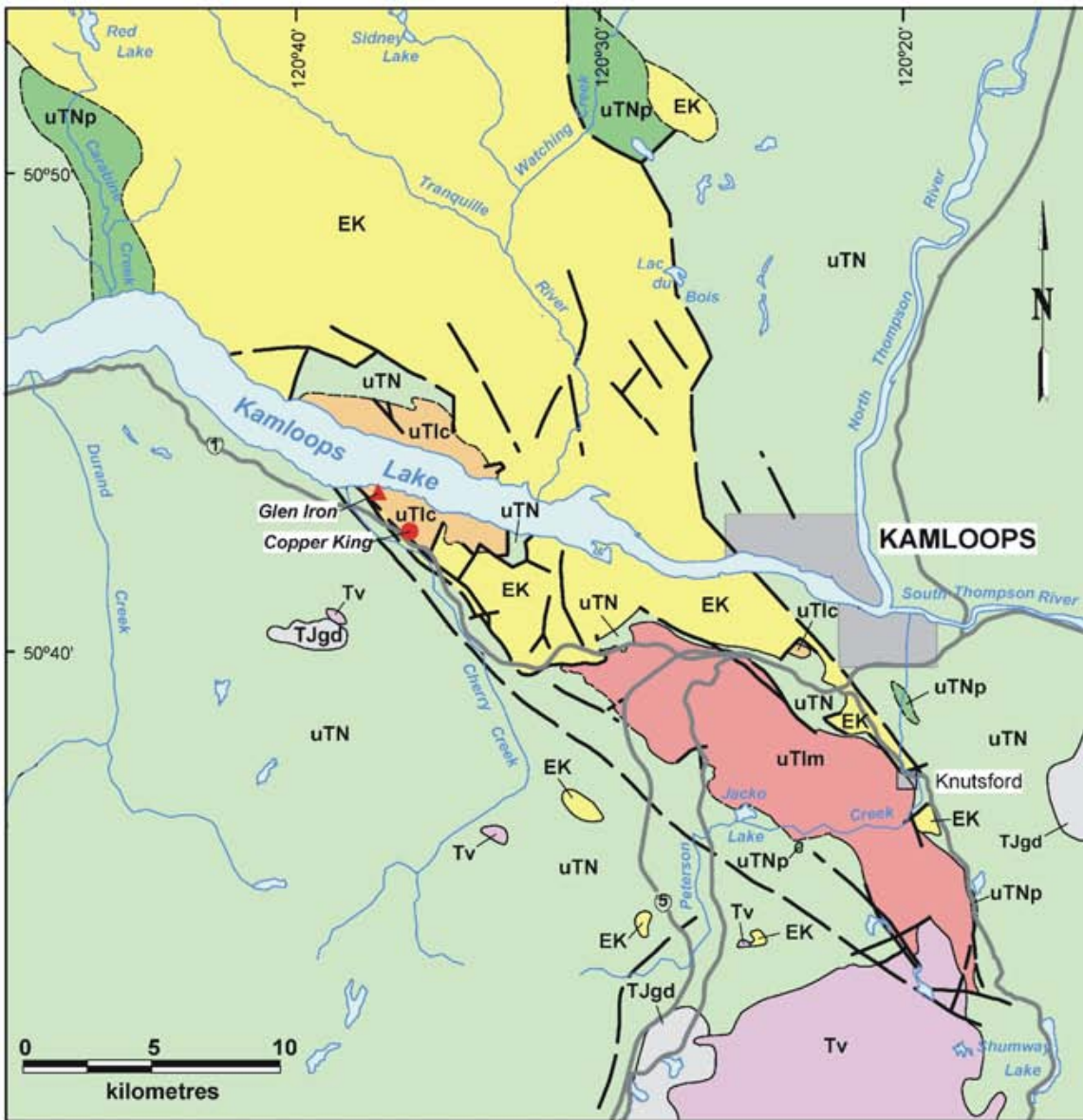
## GEOLOGICAL SETTING

The Afton mining camp near Kamloops contains a number of important copper-gold deposits, including past-producing open pit operations at Afton, the most

important deposit, Ajax East, Ajax West, Pothook and Crescent, as well as orebodies with published reserves such as Big Onion, DM and Python-Macaoo (Figs. 1 and 2). Grade and tonnage data for these and other deposits and prospects in the district are tabulated by Kwong (1987) and Ross *et al.* (1995). The most significant mineral occurrences are hosted by the Iron Mask Batholith, a northwesterly-trending composite body which intrudes volcanic, volcanoclastic and minor sedimentary rocks of the Late Triassic Nicola Group (Figs. 1 and 2). The batholith is unconformably overlain by, or in fault contact with, volcanic and sedimentary rocks of the Tertiary (Eocene) Kamloops Group (Ewing, 1981).

The geology of the Iron Mask Batholith and its ore deposits have been described by Cockfield (1948), Carr (1956), Carr and Reed (1976), Preto (1967, 1972), Northcote (1974, 1976, 1977), Hoiles (1978), Kwong (1982, 1987), Kwong *et al.* (1982), Snyder (1994), Lang and Stanley (1995), Ross *et al.* (1995) and Snyder and Russell (1993, 1995). In brief, the batholith comprises two distinct intrusive bodies, the Cherry Creek pluton, exposed around the shores of Kamloops Lake in the north, and the larger Iron Mask pluton to the south (Fig. 1). The Iron Mask Pluton comprises four major intrusive phases: the biotite-clinopyroxene-bearing Pothook diorite and related xenolith-rich, locally hornblende-bearing Hybrid unit, the Cherry Creek diorite-monzonite(-syenite) and the hornblende-phyric Sugarloaf diorite (Snyder and Russell, 1995; Fig. 2). The xenolith-bearing Hybrid unit is subdivided into several phases based on textures and clast abundance: an intrusive, xenolith-rich, heterolithic breccia (Type 1) occurring at contacts with the Nicola Group; a similar breccia with a variegated matrix in which some clasts have reacted with their host (Type 2); and a xenolith-poor breccia with a locally pegmatitic matrix containing recrystallized and digested clasts (Type 3). The Hybrid subtypes exhibit gradational contacts among themselves and with Pothook diorite which has ambiguous relationships with the Cherry Creek phase. All three units were likely emplaced penecontemporaneously, whereas the Sugarloaf diorite is considered to be marginally younger (Snyder and Russell, 1995). According to U-Pb zircon dating of the Pothook, Hybrid and Cherry Creek units, the age of the Iron Mask Batholith is approximately  $204.5 \pm 3$  Ma (Mortensen *et al.*, 1995), or latest Triassic according to the time scale of

<sup>1</sup>British Columbia Ministry of Energy and Mines



**Tertiary (Miocene?)**

**Tv** Basaltic plateau lavas

**Tertiary (Eocene)  
Kamloops Group**

**EK** volcanic, volcanoclastic and sedimentary rocks

**Late Triassic - Early Jurassic**

**TJgd** granodiorite, quartz monzonite

Geological contact

High-angle fault

▲ Magnetite deposit

**Late Triassic  
Nicola Group**

**uTNp** picritic basalt

**uTN** volcanic, volcanoclastic and sedimentary rocks

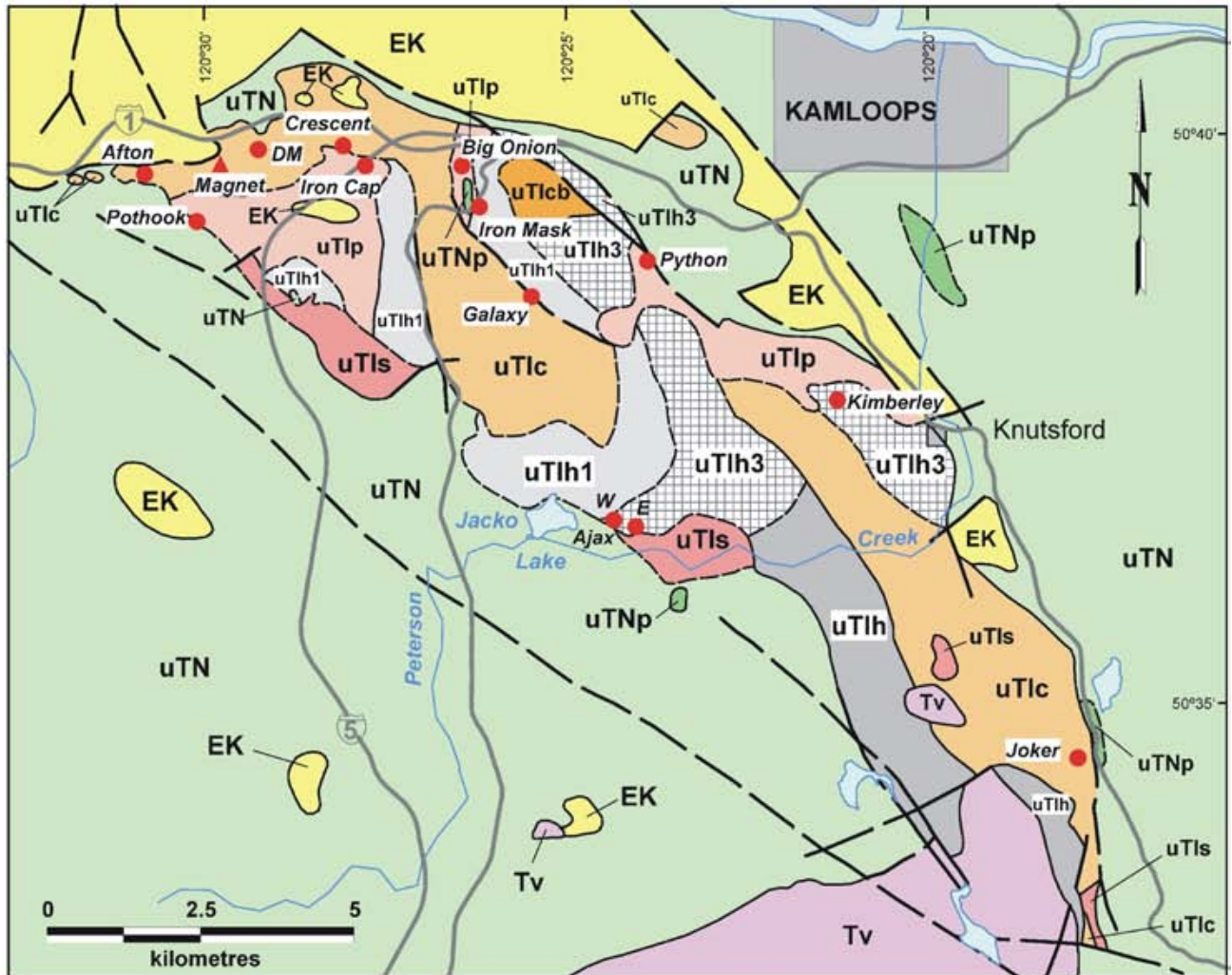
**Iron Mask Batholith**

**uTlc** Cherry Creek Pluton

**uTlm** Iron Mask Pluton

● Cu-Fe sulphide deposit

Figure 1. Regional geological setting of the Iron Mask Batholith (modified after Kwong 1987; Snyder and Russell, 1993, 1995; Snyder 1994).



**Tertiary (Miocene?)**

**Tv** Basaltic plateau lavas

**Tertiary (Eocene)**

**Kamloops Group**

**EK** volcanic, volcanoclastic and sedimentary rocks

**Late Triassic Nicola Group**

**uTNp** picritic basalt

**uTN** volcanic, volcanoclastic and sedimentary rocks

Geological contact

High-angle fault

Magnetite deposit

Cu-Fe sulphide deposit

**Late Triassic**

**Iron Mask Batholith**

**uTls** Sugarloaf diorite

**uTlcb** Cherry Creek intrusion breccia

**uTlc** Cherry Creek monzonite-diorite

**uTlh** Hybrid, undifferentiated

**uTlh3** Hybrid Unit: Type 3

**uTlh1** Hybrid Unit: Types 1 and 2

**uTlp** Pothook diorite/gabbro

Figure 2. Geology of the southern part of the Iron Mask Batholith showing the main intrusive phases and location of selected Cu-Au porphyry deposits and past-producing mines (modified after Kwong, 1987; Snyder 1994).

Palfy *et al.* (2000).

Within the Kamloops region, the Nicola Group contains picritic basalts which are particularly well exposed at Watching and Carabine creeks (Fig. 1). The most recent studies of these picrites have concluded that they represent volcanic stratigraphy conformably overlying the Nicola Group, and though locally incorporated in the Iron Mask Batholith as serpentinized xenoliths and fault slivers, are genetically unrelated to the plutonic rocks (Snyder and Russell, 1995). In this report, the picritic basalts are included within the Nicola Group.

## MINERALIZATION

Carr and Reed (1976) and Kwong (1987), among others, have pointed out that the Afton deposit appears to be unique in the Canadian Cordillera in that it is distinguished by a thick zone of supergene alteration that extends to considerable depth (up to 500 m) due to the wet climate and highly faulted and fractured nature of the orebody. These authors further noted that despite such alteration, the average grade of copper in the supergene zone is nearly equivalent to that in the hypogene zone. Although the Afton deposit generally lacks well-defined hydrothermal alteration zoning, Carr and Reed (1976) did distinguish both pyritic and magnetite-rich zones (Fig. 3). Based on detailed mineralogical observations, Kwong (1987) divided the Afton pit into a northeastern part characterized by potassium feldspar, epidote, hematite and magnetite (and minor clinopyroxene); and a southwestern portion dominated by ankeritic alteration and/or amphibole and pyrite.

The main copper-bearing minerals in the supergene zone are native copper and a sooty variety of chalcocite (in a 2:1 ratio) accompanied by minor cuprite, malachite and azurite. Hypogene sulphides are typically bornite and chalcopyrite with lesser chalcocite, and occur in veins and disseminations. To date, there are no published accounts of platinum-group minerals in the Afton deposit and little data concerning the abundance and distribution of the PGE.

## THE AFTON MINE

Prior to the start of mining operations in 1977 by Afton Mines Limited, proven reserves for the Afton orebody, the largest in the district, totalled 30.84 million tonnes grading 1.0 % Cu, 0.58 g/t Au and 4.19 g/t Ag at a cutoff grade of 0.25 % Cu (Carr and Reed, 1976). Although complex in detail, the shape of the orebody, as defined by the 0.25 % Cu cut-off grade, could be generalized as planar, striking N70°W with an average dip of 55°S and tapering downward to form a triangular-shaped zone when viewed in section from the south (Fig. 3). The upper part of the orebody prior to stripping

formed a thick supergene zone, estimated to represent approximately 80% of the mineable ore (Carr and Reed, 1976), underlain by hypogene ore (Fig. 3). The open pit resource was depleted in July 1987 after extraction of 22.1 million tonnes of ore grading 0.91 % Cu and 0.67 g/t Au (Ross *et al.*, 1995). Teck-Cominco allowed the claims to lapse in 1999 leaving a known underground mineral resource of approximately 9.5 million tonnes grading 1.5 % Cu and 1.1 g/t Au (Ross *et al.*, 1995).

Subsequently, DRC Resources Corporation acquired the ground and began a deep-drilling program in 2000 in order to evaluate the potential of the underground mineral resource beneath the open pit. By April 2002, 23,800 m of drilling had outlined a steeply dipping, southwesterly-plunging, tabular deposit passing through the southwestern corner, and extending beyond the limits, of the open pit (Fig. 4). According to a recent scoping study (October 2003), the Afton "Main Zone", as the principal orebody is known, measures 90 m in width by at least 800 m in length, and has a measured mineral resource of 9.54 million tonnes grading 1.29 % Cu, 0.94 g/t Au, 3.44 g/t Ag and 0.12 g/t Pd at a 0.7 % Cu equivalent cut-off grade; and an indicated resource of 59.16 million tonnes grading 1.05 % Cu, 0.83 g/t Au, 2.49 g/t Ag and 0.12 g/t Pd at the same cut-off. The main zone of mineralization remains open to the southwest and appears to narrow at depth and towards the surface. Further drilling is currently underway to better delineate the mineralization.

### *Potential Significance of the Picrite*

As previously noted by Carr and Reed (1976), picrites are spatially associated with (and commonly within 300 metres of) some of the largest Cu-Au deposits in the Iron Mask Batholith, notably at Afton (Fig. 4) and Ajax (Ross *et al.* 1995).

In the southwestern quadrant of the Afton pit, Kwong (1987) noted the development of an intense, pre-supergene ankeritic alteration associated with the copper mineralization. He proposed that carbonatization occurred during second boiling of a magmatic volatile phase rich in CO<sub>2</sub>, and that early ankeritic alteration could be used to identify potentially mineralized zones of magmatic-hydrothermal activity. Given the generally low CO<sub>2</sub> contents of arc magmas, a more plausible source for CO<sub>2</sub> may be the Nicola Group, where contact metamorphism and circulation of hot acidic solutions would promote the breakdown of calcium carbonate in marine sedimentary and volcanoclastic rocks. As argued by Kwong (1987), interaction of CO<sub>2</sub>-enriched, magmatic-hydrothermal fluids with highly magnesian picrite would serve to increase the pH of the fluid leading to the precipitation of Cu-Fe sulphides. This could explain the proximity of this style of alteration and mineralization to the picrite contact in the Afton pit. Moreover, the extensions of the faults that control the distribution of the picrite would also be attractive exploration targets (Fig. 4).

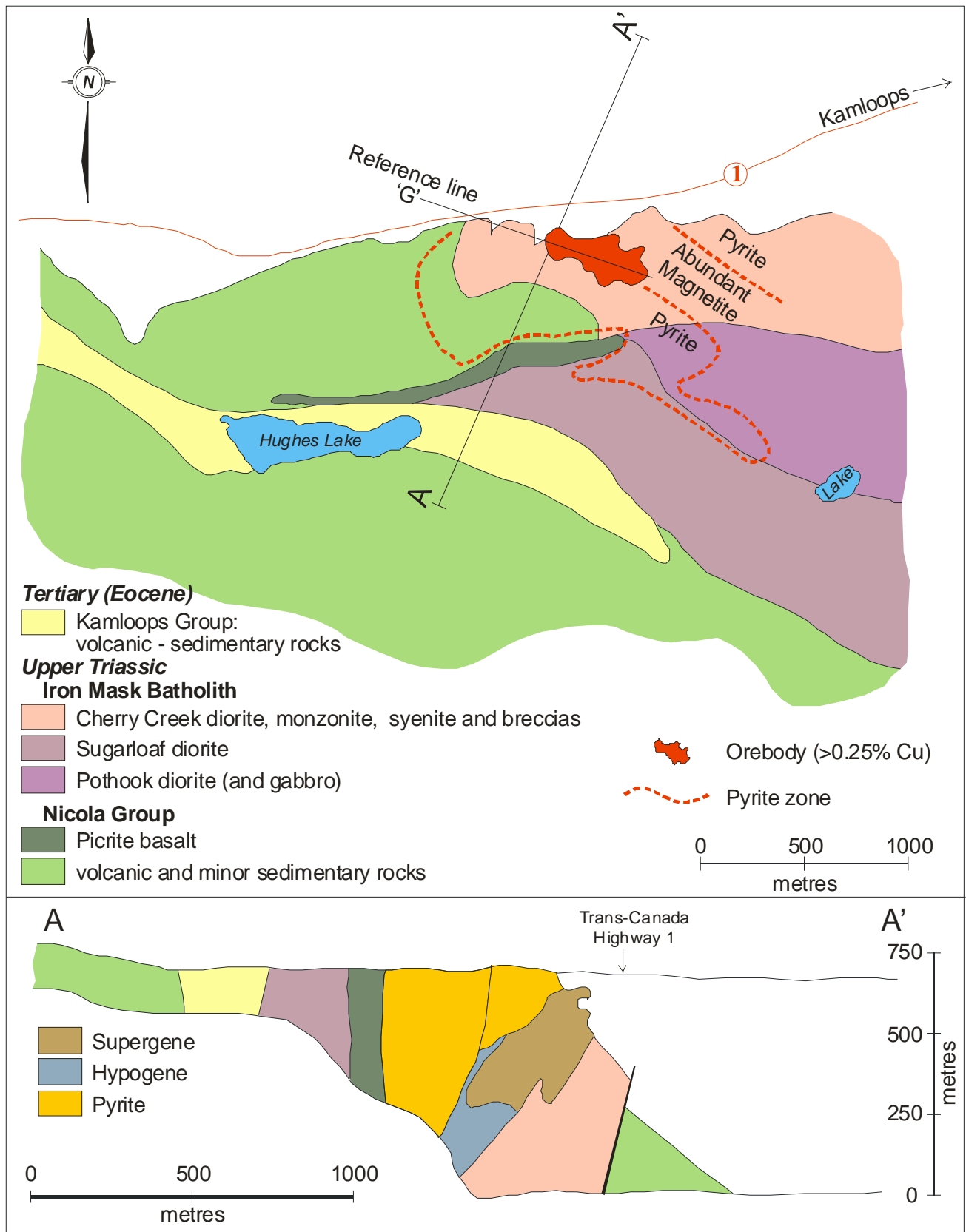


Figure 3. Simplified geological map and cross-section of the Afton property prior to mining (modified from Carr and Reed 1976).

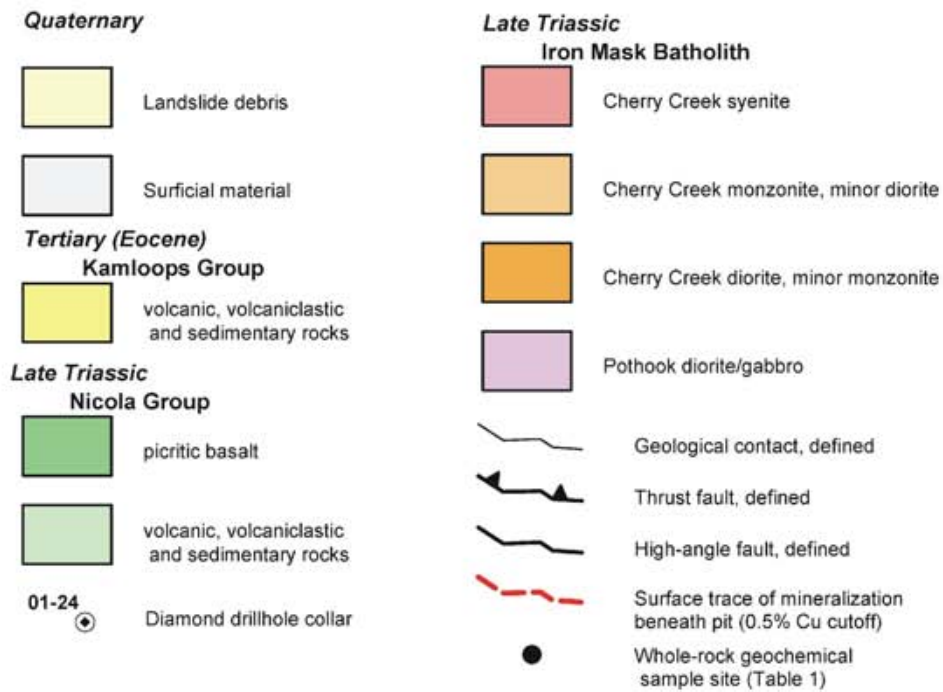
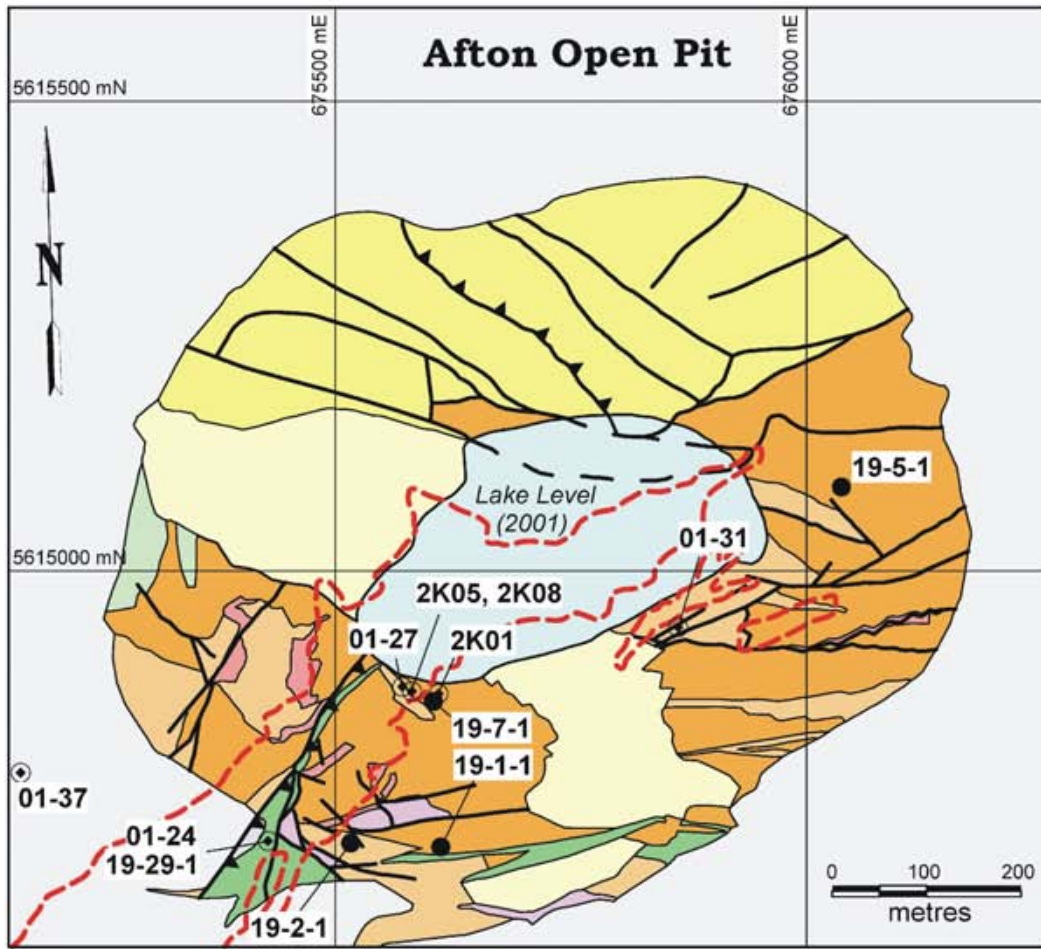


Figure 4. Geological map of the Afton open pit showing surface projection of zones of Cu-Au mineralization intersected in deep drilling and locations of samples collected from the pit and drill core (modified from a figure entitled "Afton Pit Geology Map", DRC Resources website; geology by Chris Sebert and Marek Mroczek).

The anomalously high K<sub>2</sub>O concentrations (~3 wt. %; Kwong, 1987) of picrite in the Afton pit compared to picrites in the surrounding region (~1 wt. % or less; Kwong, 1987; Snyder, 1994) indicates that the Afton picrite has experienced potassium metasomatism. The mineralogical evidence for this is represented by trace amounts of phlogopite noted in thin section by Kwong (1987). Although a minor amount of pyrite is typically present in Nicola Group rocks (including the picrite), Cu-Fe sulphides rarely penetrate more than a few centimetres into the picrite. This emphasizes the potential importance of this lithology to serve as a "chemical buffer" for the mineralizing fluids. In certain cases, therefore, the picrites may be important in localizing the site of ore deposition, but are not necessarily the only controls on sulphide mineralization.

## WHOLE-ROCK GEOCHEMISTRY

A small suite of intrusive rocks from the walls of the open pit and drill core were analyzed for major elements by x-ray fluorescence spectrometry in the Teck-Cominco Laboratories, Vancouver. The results and details of analytical methods, accuracy and precision are given in Table 1, and sample locations are shown in Figure 4.

### Sample Descriptions

The whole-rock suite includes variably altered samples of Cherry Creek diorite, syenite and leuco-monzonite dikes from the pit, and fresh hornblende monzonite from drill core (Fig. 4). The diorite is a dark greyish green, fine grained, inequigranular to microporphyritic rock containing trace amounts of sulphide and relict ferromagnesian minerals altered to chlorite and opaque oxides. The rock contains disseminated carbonate and is cut by orange-brown weathering veinlets of ankeritic carbonate. Two pale pink to greenish pink, fine-grained, leucocratic syenite dikes (~5 vol. % mafic pseudomorphs) cut Cherry Creek diorite and are themselves cut by thin carbonate veins. The syenites are partially altered to epidote-chlorite assemblages, and the dike in the eastern wall of the pit (01GNX19-5-1, Fig. 4) is clearly cut by late, northerly trending magnetite veins and dikes (<1 m in width) with epidotized envelopes. A greenish grey leuco-monzonite dike intruding Cherry Creek diorite is cut by potassium feldspar veins and traversed by fractures lined with finely crystalline pyrite. The hornblende monzonite is a pinkish grey, equigranular, medium-grained rock that is virtually unaltered.

## Results

The compositions of samples collected in the walls of the open pit have been modified to varying degrees by secondary alteration processes. For example, the extremely high loss on ignition (10.3-15.1 wt. %) for Cherry Creek diorite and a syenite dike (01GNX19-2-1) in the southern wall of the pit, proximal to the surface trace of the "Main Zone" of mineralization (Fig. 4), primarily reflects loss of CO<sub>2</sub> due to intense carbonate alteration. These samples also have anomalously low silica, alumina and alkalis. Mobility of alkalis is also evident in the leuco-monzonite dike (Na<sub>2</sub>O/K<sub>2</sub>O = 7), which is exposed at the same locality.

The CIPW-normative compositions of rocks from the Afton pit and Iron Mask Batholith in general are plotted in the IUGS classification scheme in Figure 5. This

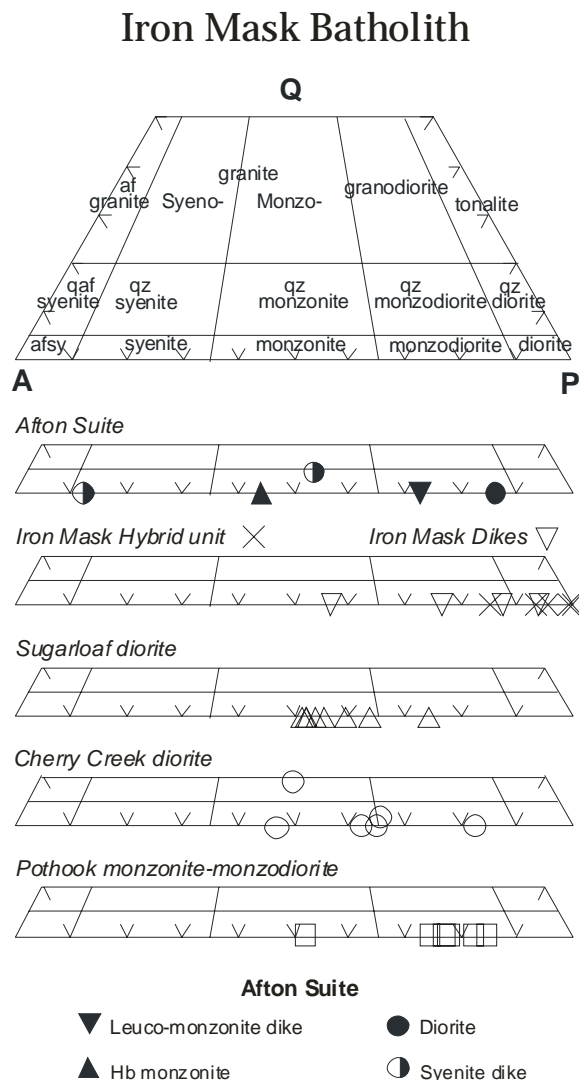


Figure 5. CIPW-normative compositions (wt. %) of the Afton pit suite and plutonic rocks from the Iron Mask Batholith (Snyder 1994) plotted in the QAP classification scheme of Le Maitre (1989) using the projection parameters of Le Maitre (1976).

TABLE 1: MAJOR ELEMENT WHOLE-ROCK ANALYSES OF SELECTED PLUTONIC ROCKS, AFTON PIT

Sample	Rock Type	UTM Zone 10 (NAD 83)		wt. %											Sum	
		Easting	Northing	SiO <sub>2</sub>	TiO <sub>2</sub>	Al <sub>2</sub> O <sub>3</sub>	Fe <sub>2</sub> O <sub>3</sub>	FeO	MnO	MgO	CaO	Na <sub>2</sub> O	K <sub>2</sub> O	P <sub>2</sub> O <sub>5</sub>		LOI
01GNX19-1-1	Diorite	675614	5614714	40.65	0.64	9.71	5.43	6.35	0.25	15.15	7.92	1.01	0.55	0.21	10.30	98.17
01GNX19-2-1	Syenite dike	675517	5614714	47.48	0.70	11.60	1.88	2.82	0.07	5.80	8.68	2.58	2.03	0.76	15.14	99.52
01GNX19-5-1	Syenite dike	676037	5615089	58.13	0.40	17.04	2.05	0.31	0.10	1.47	4.34	3.07	8.63	0.18	3.37	99.08
01GNX19-7-1	leuco-monzonite dike	675605	5614875	56.77	0.55	18.20	1.22	1.89	0.07	3.60	4.44	7.05	0.97	0.23	4.66	99.65
01GNX19-29-1	Hornblende monzonite (DDH01-24 352.2m)	675429	5614712	52.55	0.62	18.43	4.31	2.38	0.09	2.83	7.13	3.78	4.36	0.44	2.42	99.35
<u>Quality Control</u>																
Std SY 4 *				49.77	0.28	20.60	3.14	2.70	0.10	0.51	8.02	7.03	1.64	0.12	5.07	98.99
CANMET SY 4**				49.90	0.29	20.69	2.86	3.45	0.11	0.54	8.05	7.10	1.66	0.13	4.56	99.34
% Difference				0.3	2.5	0.4	9.5	24.2	7.7	5.7	0.4	1.0	1.2	8.8	10.5	
01GNX10-4-1				56.93	0.87	14.92	2.72	3.01	0.07	3.85	3.94	3.17	4.19	0.51	4.96	99.15
01GNX10-4-1D				56.90	0.87	15.05	2.69	2.99	0.07	3.92	3.78	3.22	4.19	0.51	4.90	99.09
% Difference				0.1	0.0	0.9	1.1	0.9	0.0	1.8	4.1	1.6	0.0	0.0	1.3	

Samples were jaw crushed (steel) and pulverized in a tungsten carbide swing mill and analyzed by x-ray fluorescence at Teck-Cominco Laboratories using a lithium tetraborate fused bead for major elements (Norrish and Hutton, 1969). Loss on ignition (LOI) was measured gravimetrically at 1100 °C. D, duplicate analysis; \* hidden standard % Difference =  $ABS((x1-x2)/(x1+x2)/2) \times 100$

\*\* CANMET recommended value (anhydrous basis; Bowman, 1995). FeO determined by titration and Fe<sub>2</sub>O<sub>3</sub> by difference from total Fe as Fe<sub>2</sub>O<sub>3</sub>

projection permits a direct comparison between modal and normative classification schemes since rocks containing normative feldspathoids plot on the A-P join. Small amounts of feldspathoids do occur in the CIPW norms of some of the least altered batholithic rocks (0-5% normative *ne* and 0-3% *lc* assuming  $\text{Fe}_2\text{O}_3 = 0.15$  total Fe as FeO) and samples from the Afton pit (0-3.5% *ne*). To date, however, feldspathoids have not been identified in thin section. Modal quartz (<3 vol. %) that appears to be primary in origin is comparatively rare but has been detected locally (Snyder, 1994), and normative *qz* is typically lacking except in altered samples. An altered syenite dike from the Afton pit, for example, contains 2.5% *qz*.

As shown in the QAP plot (Fig. 5), most rocks comprising the Iron Mask Batholith are monzonites, monzodiorites and diorites. The Pothook phase is predominantly dioritic whereas the younger Sugarloaf "diorite" shows a bias towards monzonite. The two least altered rocks in the Afton pit suite fall in the monzonite and syenite fields in accordance with their mineralogy. It is not clear from either its major element chemistry or mineralogy whether the hornblende monzonite encountered in drill core belongs to the Cherry Creek or Sugarloaf suites.

In an alkalis vs silica diagram (Fig. 6), the Iron Mask suite forms a linear compositional trend that lies just within the alkaline field. Very few rock compositions plot on the subalkaline side of the discriminant, and these include the highly altered samples from the Afton pit. In

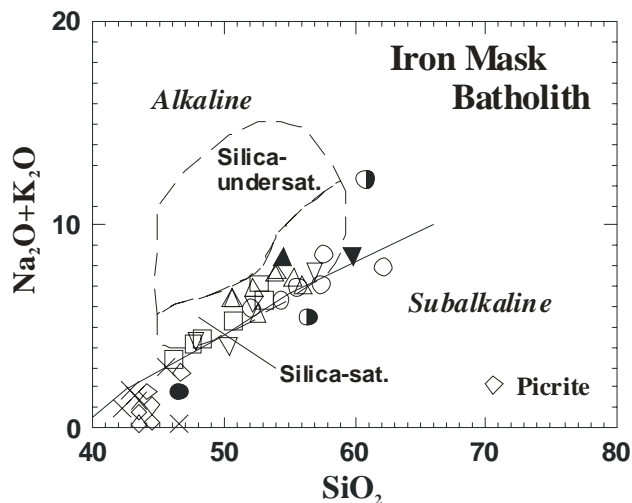


Figure 6. Alkalis vs silica (wt. %) plot for the Afton pit suite, Iron Mask Batholith and picritic basalts (Snyder 1994) showing the discriminant of Irvine and Baragar (1971) between subalkaline and alkaline rock types. Also shown are the fields of Lang *et al.* (1994, 1995) for silica-saturated and silica-undersaturated intrusions associated with alkaline Cu-Au porphyry deposits. Symbols as for Fig. 5. All rock compositions are plotted on an anhydrous basis normalized to 100 wt. % with total iron as FeO.

terms of the classification of Lang *et al.* (1994, 1995), the suite shows a distinct affinity towards the silica-saturated subclass of plutonic rocks associated with Cu-Au porphyry deposits.

An alkalis-FeO-MgO (AFM) plot (Fig. 7) shows the strong iron-enrichment of the Iron Mask suite and a marked enrichment in alkalis with differentiation. Altered rocks from the Afton pit lie below this trend with the exception of the least altered syenite dike which is more enriched in alkalis than the rest of the suite (cf. Fig 6).

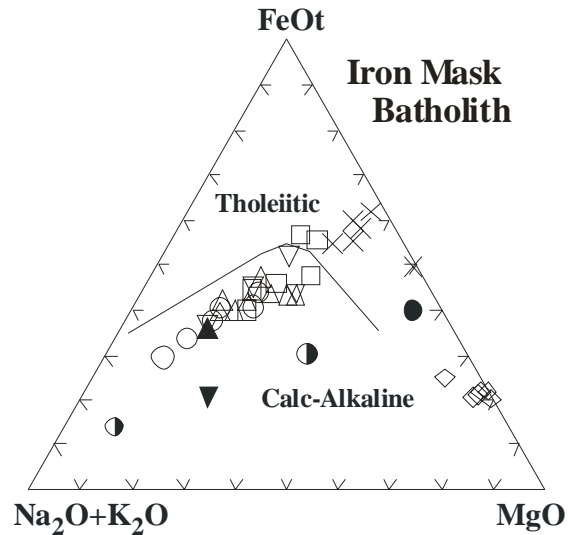


Figure 7. Alkalis-total iron-magnesia (AFM) plot (wt. %) for rocks of the Afton pit suite, Iron Mask Batholith and picritic basalts (Snyder 1994) showing the discriminant of Irvine and Baragar (1971) between the calc-alkaline and tholeiitic fields for subalkaline rocks. The discriminant is shown for reference only, not for classification purposes. Symbols as for Fig. 5. All rock compositions are plotted on a normalized anhydrous basis with total iron as FeO.

## PGE MINERALIZATION

A suite of 12 samples of well-mineralized drill core, collected within intervals previously determined by DRC Resources staff to carry anomalously high abundances of Pd and/or Pt, was selected for petrographic study and PGE analysis using both conventional fire assay and multi-element acid digestion methods with an ICP-ES/MS finish. Prior to the most recent phase of exploration at Afton, abundances of PGE in the Cu-Fe sulphide ores were poorly known. For example, Kwong (1987) reported detectable abundances of palladium (0.10-0.15 ppm Pd by emission spectrographic analysis) in mineralized samples from the Afton pit, and a single highly anomalous specimen of fine-grained, carbonate-altered diorite with veins of chalcopyrite returned 0.34 ppm Pd (0.34 g/tonne). The ppb to sub-ppb levels of detection for the PGE combined with the high precision of modern analytical techniques permits the concentrations of PGE in the mineralized rocks to be accurately determined and

enables a preliminary assessment of potential "pathfinder" elements in PGE-enriched Cu-Au porphyry systems.

### **Sample Descriptions**

Mineralized samples examined in this study primarily represent drill core from the Cherry Creek unit; however, samples of a pyrite-bearing picritic basalt and a massive magnetite vein are also included. Their principal textural and mineralogical features are described below. More detailed descriptions are given in the Appendix and drillhole locations are shown in Figure 4.

The main host of mineralization in the sample suite is a diorite or leuco-diorite with microporphyritic to inequigranular textures (Photos 1 and 2). Euhedral to subhedral, turbid plagioclase, locally preserving albite twins, forms subequant to lath-like phenocrysts (0.8-3 mm) that rarely exhibit a primary magmatic flow alignment. Relict mafic minerals (amphibole?) are generally sparse (<5 vol. %) and typically pseudomorphed by a fine-grained intergrowth of chlorite/biotite, opaques oxides and leucoxene. Minor quartz forms anhedral crystals in the groundmass that may exhibit subgrain mosaic boundaries; most quartz does not appear to be of primary origin. Due to the extent of potassic alteration in these rocks (discussed below), the amount of primary potassium feldspar, which is confined to the groundmass, is difficult to estimate. Mineralogically, the original rock composition appears to be best described as leuco-diorite or monzodiorite.

Secondary minerals include biotite, chlorite, sericite, epidote, quartz, carbonate (calcite-dolomite-ankerite), apatite, magnetite, hematite, limonite and clay minerals. The principal alteration assemblage is represented by an early potassic or (calcic)-potassic alteration involving biotite-sericite-alkali feldspar-quartz accompanied by minor epidote (Photos 3 and 4). Secondary biotite typically forms tiny (<0.1 mm), deep reddish brown crystals that may be partially altered to pale green, weakly pleochroic chlorite. Fine-grained sericite accompanied by clay minerals preferentially replaces plagioclase. Apatite is not a common accessory phase, but in one sample of magnetite-apatite-carbonate-sulphide breccia it locally forms monomineralic aggregates of large grains (<0.8 mm) with abundant opaque inclusions. Late veins of carbonate-quartz+/-sulphide cut this early potassic alteration, and carbonatization may locally be pervasive.

The principal sulphide minerals in the sample suite are chalcopyrite, bornite, chalcocite, native copper and pyrite. Two core specimens collected one metre apart in the same drillhole (224-225m, drillhole 2K08, Fig. 4) contain disseminations and veins of native copper and chalcocite, respectively (01GNX19-10-1 and 19-9-1; see Appendix), and attest to the depth reached (locally) by supergene alteration processes (>400 m below the rim of the pit). The remaining sulphide samples are characterized by hypogene assemblages involving mainly chalcopyrite

and bornite accompanied by minor chalcocite and pyrite. These copper sulphides locally show incipient alteration to covellite, digenite, malachite and azurite.

Pyrite enclosed by silicates is generally euhedral to subhedral, but typically assumes rounded to embayed habits against Cu-Fe sulphides, which locally occupy fracture fillings (Photos 5 and 6). These textures are indicative of replacement of early pyrite by Cu-Fe sulphide mineralization, and may account for the apparent rarity of pyrite at depth relative to near surface environments (Fig. 3). Both chalcopyrite- and bornite-dominant ores exist, as well as ores with subequal proportions of each where both sulphides apparently crystallized in equilibrium with quartz (Photo 7). Traces of chalcopyrite enclosed in silicates within bornite-dominant ores possibly reflect an earlier chalcopyrite mineralization event (Photo 8).

Textural relationships between secondary silicate assemblages and Cu-Fe sulphides indicate that mineralization accompanied potassic or (calcic)-potassic alteration. For example, faceted crystals of neocrystic alkali feldspar, quartz, biotite, and, to a lesser extent, epidote, locally line replacement cavities or occur as inclusions within, and intergrowths with, the sulphides (Photos 3, 4 and 7). Although both chalcopyrite and bornite are found in veins, their most prevalent mode of occurrence is one of irregular, patchy replacements, fine disseminations and blebs. The sulphides preferentially replace the fine-grained groundmass of microporphyritic diorites (rarely plagioclase phenocrysts) and thus superficially impart a "pseudo-magmatic" interstitial texture to the rock (Photos 1 and 2). However, the intricate nature of sulphide-silicate contacts, and the presence of intimately associated, potassic and (calcic)-potassic alteration assemblages, serve to distinguish these textures from those characteristic of orthomagmatic sulphide deposits. Kwong (1987) also noted that the disseminated sulphides are commonly accompanied by biotite and described them as interconnected impregnations rather than "isolated globules".

A massive to semi-massive magnetite vein (0.5 m wide) cutting Cherry Creek diorite was sampled in the eastern wall of the pit approximately 15 metres north of the syenite dike locality (01GNX19-5-1, Fig. 4). In thin section, the magnetite is locally intergrown with granular epidote and minor to trace amounts of chlorite and apatite, and no sulphides were observed. The presence of finely interlaced and branching magnetite veinlets at the margins of this body within a distinct envelope of epidote(-chlorite) alteration are features consistent with a hydrothermal origin.

A dark grey-green serpentized and variably oxidized picritic basalt is exposed in the southwestern corner of the Afton pit where it is in fault contact with Cherry Creek rocks along steep northeasterly trending structures (Fig. 4). Weathering appears responsible for the locally nodular outcrop character noted by Kwong (1987). In thin section, faceted to rounded phenocrysts (<3 mm)

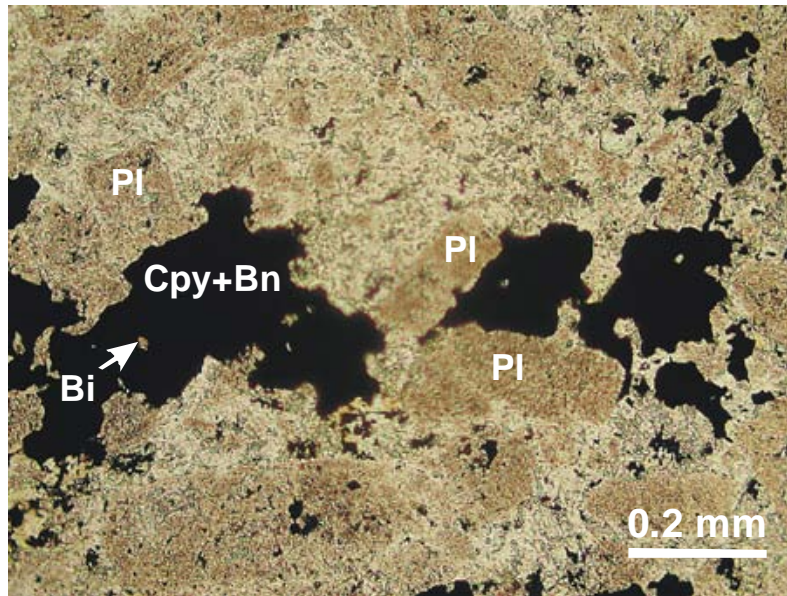


Photo 1. Disseminated chalcopyrite (Cpy) and bornite (Bn) preferentially replacing the groundmass in microporphyritic diorite. Plagioclase (Pl) phenocrysts are partially altered to clay-sericite. Note minute brown biotite (Bi) enclosed in sulfide. (Plane-polarized light; 01GNX19-11-1).

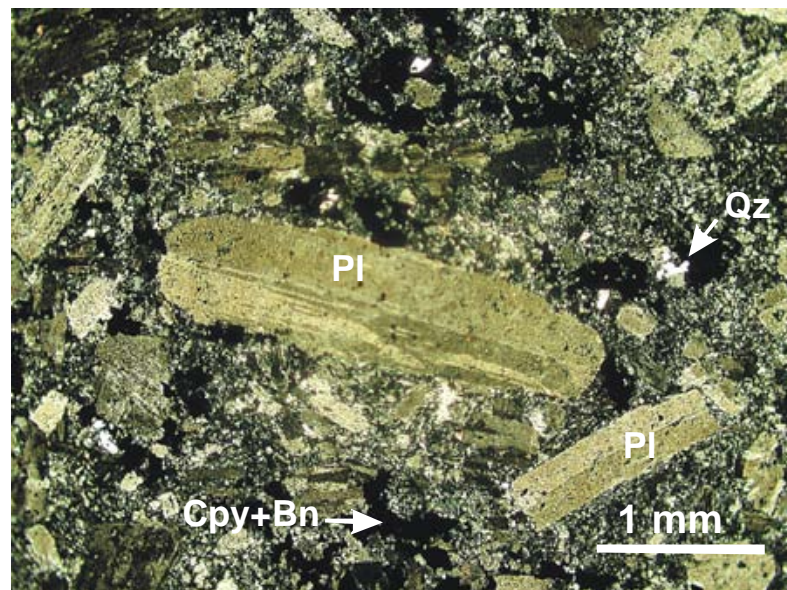


Photo 2. Disseminated chalcopyrite (Cpy) and Bornite (Bn) preferentially replacing the groundmass in microporphyritic diorite. Plagioclase (Pl) phenocrysts are partially altered to clay-sericite. Note tiny quartz (Qz) crystals locally associated with sulfide. (Crossed nicols; 01GNX19-11-1).

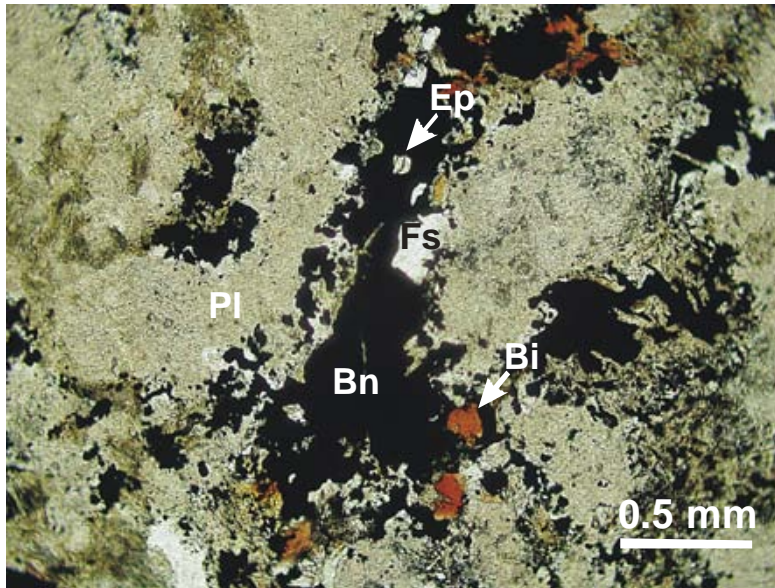


Photo 3. Bornite (Bn) in irregular veins and patchy replacements associated with alkali feldspar (Fs), reddish-brown biotite (Bi) and trace amounts of epidote (Ep). Potassic-altered diorite with sericitized plagioclase (Pl). (Plane-polarized light; 01GNX19-15-1) .

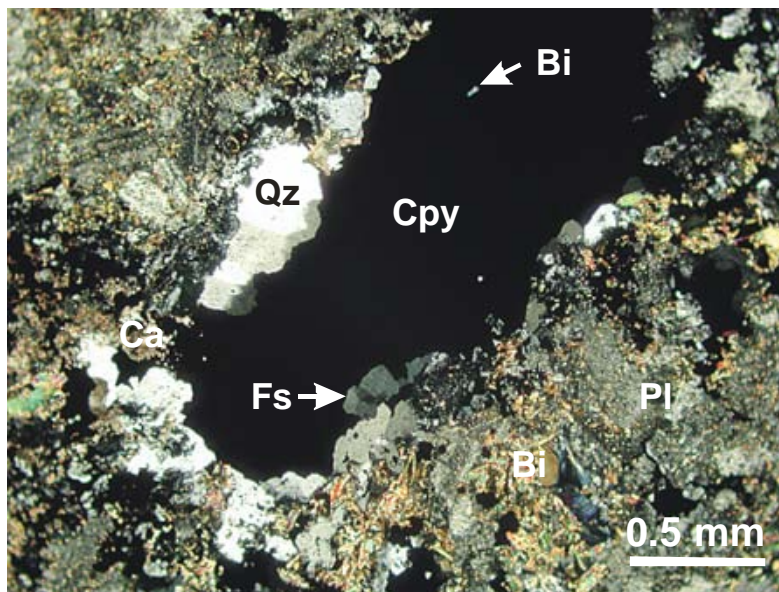


Photo 4. Irregular veins and disseminations of chalcopyrite (Cpy) intergrown with quartz (Qz), biotite-chlorite and minor carbonate (Ca). Plagioclase (Pl) in the diorite host has been partially altered to biotite (Bi) and lesser sericite. (Crossed nicols; 01GNX19-21-1).

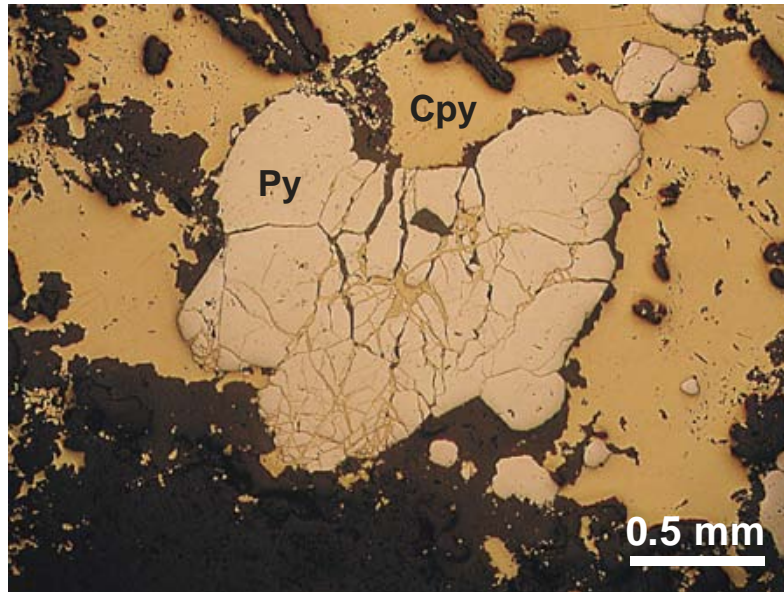


Photo 5. Crystals of pyrite (Py) veined by chalcopyrite (Cpy) and secondary silicates (biotite, alkali feldspar and quartz), calcite and minor apatite. (Reflected plane-polarized light; 01GNX19-21-1).

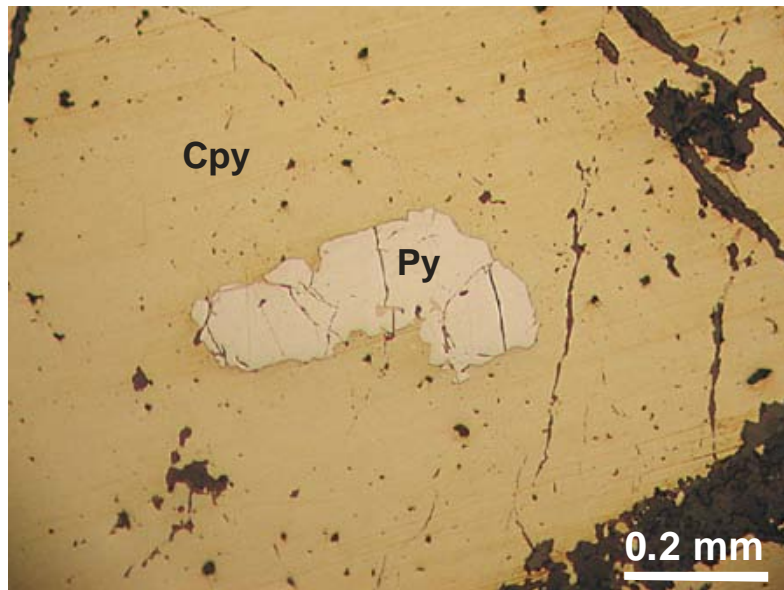


Photo 6. Intricately resorbed pyrite (Py) enclosed in chalcopyrite (Cpy) within sulphide bleb in magnetite-carbonate-sulphide-apatite vein breccia cutting diorite/monzonite. (Reflected plane-polarized light; 01GNX19-26-1).

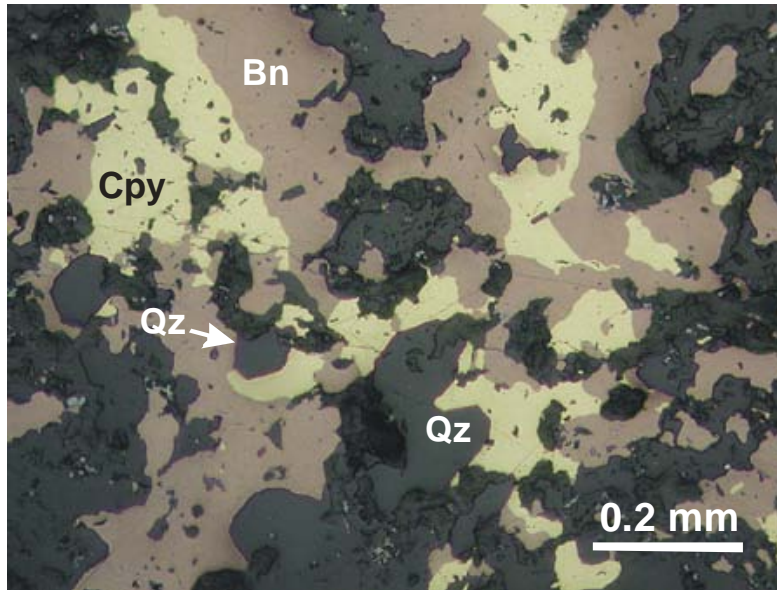


Photo 7. Disseminated chalcopyrite (Cpy) and bornite (Bn) in the groundmass of microporphyritic diorite. Note euhedral quartz (Qz) crystals intergrown with sulfide. (Reflected plane-polarized light; 01GNX19-11-1).

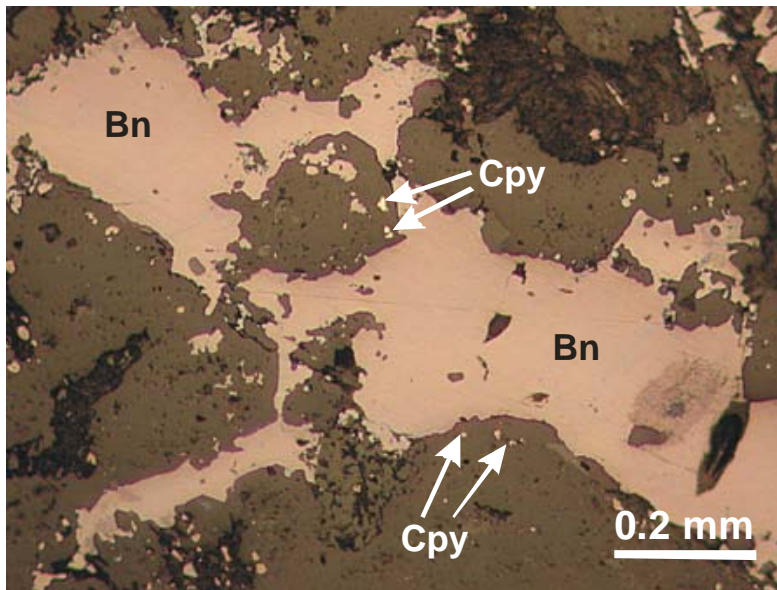


Photo 8. Veins and disseminations of bornite (Bn) associated with variably chloritized, reddish-brown biotite (Bi), alkali feldspar and trace epidote and chalcopyrite (Cpy). Potassic-altered microdiorite. (Plane-polarized light; 01GNX19-15-1).

of fresh clinopyroxene and altered olivine are enclosed in a fine-grained groundmass of feldspar, opaque oxides and secondary alteration products. Olivine is completely pseudomorphed by a felted mixture of magnetite, serpentine and tremolite-actinolite; the latter mineral is also common in the groundmass. A core sample containing small amounts of euhedral to subhedral pyrite (<1 vol. %) was collected for analysis (01GNX19-4-1, drillhole 2K01, Appendix and Fig. 4). The presence of tremolite-actinolite alteration indicates that the picrite is older than the mineralization event, consistent with observations made at the Ajax pits and elsewhere in the Iron Mask Batholith (Ross *et al.*, 1995; Lang and Stanley, 1995).

### Lithochemical Assays

The results of lithochemical analyses for the PGE and other elements are presented in Table 2 which includes descriptions of the host rock, mineralization and alteration assemblages. All samples were crushed in a hardened-steel jaw crusher and powdered in a tungsten carbide swing mill. A quartz wash was done between samples to avoid cross-contamination. Splits of the rock powders were analyzed by Acme Laboratories, Vancouver, using conventional fire assay and aqua regia digestion. Accuracy and precision were monitored by including hidden duplicates and international and in-house reference materials in the run (*see* Table 2).

A comparison of the analytical techniques for Pt, Pd and Au is shown in Figure 8. There is good reproducibility for Pd between the two methods whereas Pt abundances are systematically under-reported by aqua regia digestion. A similar discrepancy was noted previously for mineralized samples from the Sappho property which attain much higher platinum concentrations (up to 8500 ppb Pt; Nixon, 2002). The results for gold exhibit a near-normal distribution about the 1:1 line of perfect agreement between the analytical methods. The scatter is attributed to a "nugget" effect caused by the presence of finely crystalline native gold.

The abundances of Pd, Pt and Au in the sample suite range 5-3833 ppb, 0.2-143 ppb (fire assay) and <1-13905 ppb, respectively (Table 2). Note the large differences that exist in gold determinations on the same sample which, as noted above, is considered to reflect sample inhomogeneity. The determination of Rh by the fire assay technique is only semi-quantitative due to partial loss by volatilization; therefore, Rh values given in Table 2 are probably best regarded as minimum abundances.

Samples enriched in Cu-bearing minerals have the following range of abundances: 19-3833 ppb Pd, <3-143 ppb Pt and 1226-13905 ppb Au. Palladium approaches or exceeds 1 g/t in four samples; the three most Pd-rich contain chalcopyrite in disseminations and veinlets, and the fourth carries bornite (Table 2). All these highly

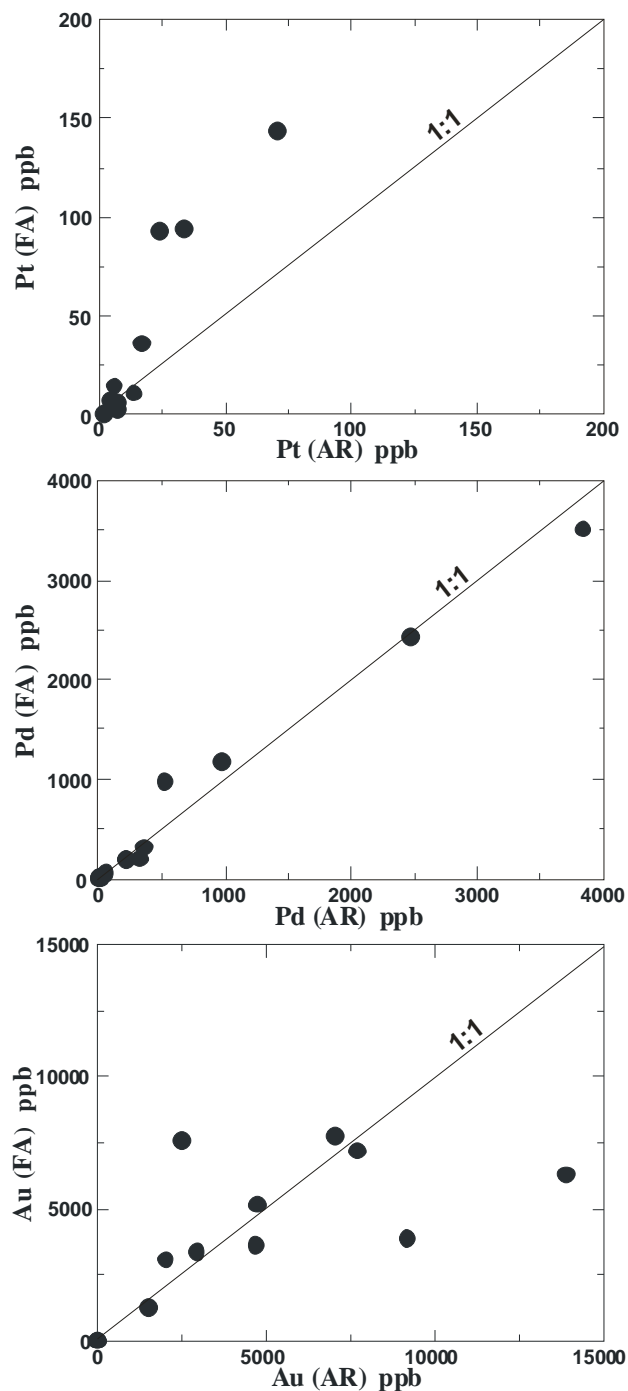


Figure 8. Comparison of analytical methods for platinum-group elements and gold. FA, fire assay; AR, aqua regia digestion. Note the systematic bias towards lower Pt values returned by the aqua regia digestion method.

anomalous samples are from the hypogene zone. Given that the average grade for the measured and indicated mineral resource at Afton is approximately 0.12 g/t Pd, it is apparent that zones anomalously enriched in palladium exist within the ore body. Pt abundances are generally low yielding high Pd/Pt ratios in the PGE-enriched zones. Gold is uniformly high, as expected, reaching 13.9 g/t. Copper abundances range from 1.1 to 7.9 wt. %, and all

**TABLE 2: LITHOGEOCHEMICAL ASSAYS OF MINERALIZED ROCKS, AFTON MINE**

Sample	DDH (Box)	Depth (m)	Rock Type	Mineralization/Alteration	wt. %										
					Ti	Al	Fe	Mg	Ca	Na	K	P	S		
01GNX 19-6-1***	Afton pit	outcrop	massive Mt vein	Mt vein (Ep+Chl+Ap)	0.07	0.48	34.45	0.88	0.63	0.02	0.01	0.01	0.01	0.02	
01GNX 19-4-1	2K01(25)	23.35	Ol-Cpx-phytic basalt (Picrite)	(dissem Py); Tr-Act (Sp)	0.12	3.17	3.41	6.03	1.00	0.09	3.12	0.21	0.21	<.01	
01GNX 19-10-1	2K05(37)	224.20	microporphyrific Qz-bearing diorite	sparse native Cu+Hm; clay (Ser)	0.00	0.79	1.49	0.11	0.30	0.10	0.37	0.14	<.01		
01GNX 19-9-1	2K05(37)	225.20	microporphyrific (leuco)diorite	Cc dissem & veinlets; clay+Ca (Ser)	0.00	0.78	2.00	1.42	3.24	0.08	0.35	0.10	1.29		
01GNX 19-36-1	2K08(19)	142.50	inequigranular (leuco)diorite	Bn (Cpy+Cov+?Dg); Ser+clay+Ca	0.00	0.74	2.11	2.84	7.12	0.06	0.16	0.71	1.13		
01GNX 19-26-1	01-24(62)	349.80	diorite	Cpy (Py) blebs; Mt+Ca (Fs+Ap)	0.01	0.68	21.09	1.67	4.66	0.02	0.01	2.01	3.98		
01GNX 19-32-1	01-27(44)	334.30	microporphyrific diorite	dissem Cpy (Mt); Ser+Bi+Fs+Chl	0.07	1.66	7.50	2.29	3.06	0.06	0.50	0.19	3.81		
01GNX 19-14-1	01-27(45)	241.80	microporphyrific diorite	Cpy dissem & fractures; Ser+Ca (Hm+Chl+Ap)	0.00	1.46	3.62	1.95	1.82	0.11	0.19	0.18	1.35		
01GNX 19-15-1	01-31(06)	33.80	inequigranular diorite	dissem Bn; Ser+Bi (Fs+clay+Ep+Chl)	0.12	1.39	2.55	1.55	1.49	0.13	0.19	0.13	2.48		
01GNX 19-22-1	01-37(73)	411.40	microporphyrific diorite	dissem Cpy (+Cc); Ser+Ca (Fs+Bi)	0.02	0.98	3.24	2.34	4.06	0.08	0.41	0.14	0.91		
01GNX 19-21-1	01-37(73)	413.50	inequigranular (leuco)diorite	Cpy (Py) dissem & veinlets; Ser+Bi (Ca)	0.08	1.19	4.87	2.70	4.24	0.05	0.44	0.19	2.18		
01GNX 19-31-1	01-37(74)	419.50	microporphyrific diorite/monzonite	Cpy dissem & veinlets; Ser+Bi (Fs+Chl+Cat+Ap+clay)	0.06	1.44	4.68	2.30	1.21	0.06	0.25	0.13	2.72		
<u>Quality Control</u>															
01GNX 19-9-1					0.00	0.78	2.00	1.42	3.24	0.08	0.35	0.10	1.29		
01GNX 19-9-1D					0.00	0.83	2.02	1.45	3.29	0.09	0.33	0.11	1.24		
% Difference						6	1	2	2	7	6	12	4		
01GNX 12-2-5					0.06	0.81	29.20	0.22	3.76	0.02	0.37	1.81	25.94		
01GNX 12-2-5D					0.07	0.85	28.16	0.21	3.77	0.02	0.33	1.65	21.57		
% Difference					8	5	4	5	0	0	11	10	18		
GSB Std. OC-80					0.09	1.39	4.43	1.35	0.84	0.02	0.13	0.15	0.01		
GSB Std. OC-80					0.09	1.71	4.80	1.45	0.90	0.02	0.17	0.18	0.02		
% Difference					1	21	8	7	7	6	27	18	67		
Std WMG-1					0.13	2.73	7.55	2.60	2.12	0.01	0.02	0.06	2.91		
Std WMG-1						4.40	11.89	7.15	10.70						
% Difference						47	45	93	134						

TABLE 2. CONTINUED

Sample	B	Sr	Ba	Th	U	La	Mn	Sc	V	Cr	Ni	Co	Cu	Mo	Pb	Zn	As	Sb	Bi	Tl	Ga	Cd	Se	Te
01GNX 19-6-1***	<1	30	41	0.5	0.1	1.0	1845	1.1	1032	11	126	90	968	0.71	0.70	110	9	0.25	<.02	<.02	9.0	0.02	0.1	<.02
01GNX 19-4-1	<1	47	202	0.6	0.2	2.6	361	1.5	82	820	526	18	9	0.95	0.01	20	3	<.02	<.02	0.26	6.8	<.01	0.2	0.03
01GNX 19-10-1	<1	98	275	0.3	0.2	1.1	108	9.8	29	23	8	2	43815	0.53	6.9	99	75	64	0.46	<.02	2.2	0.11	7.1	0.46
01GNX 19-9-1	<1	61	49	0.5	0.5	4.0	3558	12.3	105	21	24	17	58400	4.33	28.97	443	333	222.9	0.76	<.02	3.1	3.39	23.5	0.40
01GNX 19-36-1	<1	98	78	1.3	0.8	12.5	1401	3.8	134	18	23	5	41527	3.25	12	56	14	0.66	1.22	<.02	3.3	0.81	34.5	0.65
01GNX 19-26-1	<1	39	37	1.3	0.5	8.3	2325	2.6	954	21	204	45	72641	6.36	29.04	180	504	31.04	7.22	0.17	8.5	0.98	39.8	0.14
01GNX 19-32-1	<1	56	42	0.8	0.1	4.6	1045	12.4	109	11	70	19	41568	25.7	2.64	70	48	6.77	0.29	<.02	7.4	0.13	21.1	0.31
01GNX 19-14-1	3	33	31	0.6	0.2	3.0	1629	7.1	103	70	51	16	16292	9.81	1.7	90	109	5.46	0.15	0.02	7.8	0.03	16.6	0.13
01GNX 19-15-1	<1	109	53	0.4	0.5	3.1	692	5.4	114	21	43	9	79322	46.36	212.4	99	1	0.53	0.97	<.02	6.5	11.23	18.0	0.28
01GNX 19-22-1	10	64	62	1.1	0.1	9.0	772	13.0	107	31	141	29	10830	1.38	4.0	38	97	3.44	0.18	0.03	4.5	0.19	9.0	0.05
01GNX 19-21-1	4	57	78	0.7	<.1	4.7	869	15.8	166	41	185	29	23117	2.03	3.6	55	73	1.85	0.52	0.03	6.7	0.22	22.2	0.09
01GNX 19-31-1	2	23	54	0.5	<.1	2.1	565	8.1	126	58	233	66	28142	1.81	1.8	47	76	1.58	0.39	0.02	8.9	0.20	18.0	0.12
<b>Quality Control</b>																								
01GNX 19-9-1	<1	61	49	0.5	0.5	4.0	3558	12.3	105	21	24	17	58400	4.33	28.97	443	333	222.9	0.76	<.02	3.1	3.39	23.5	0.40
01GNX 19-9-1D	<1	63	45	0.5	0.5	3.6	3600	10.8	92	18	24	16	59271	3.92	30	452	317	202	0.91	<.02	2.8	3.17	22.8	0.41
% Difference		3	9	0	0	11	1	13	13	14	0	5	1	10	3	2	5	10	18		10	7	3	2
01GNX 12-2-5	-1	673	18	28.8	2.5	337.3	456	-0.1	55	20	330	477	76480	18.71	13.68	2634	31.6	2.93	2.86	0.09	2.4	64.64	120	0.62
01GNX 12-2-5D	-1	616	17	24.4	2.2	276.1	504	-0.1	51	25	298	441	71339	16.68	12.54	2521	25.2	2.64	2.42	0.08	2.3	50.81	96.9	0.58
% Difference		0	8	17	13	20	10	0	8	21	10	8	7	11	9	4	23	10	17	12	4	24	21	7
GSB Std. OC-80	1	49	67	1	0	7	743	4	136	72	38	23	59	1	3	51	5	1	0	0	5	0	0	0
GSB Std. OC-80	<1	55	67	1.1	0.3	8.1	813	4.4	142	86	42	25	59	0.54	3.97	57	5.6	0.41	0.04	0.04	5.3	0.14	0.3	0.02
% Difference		11	0	9.524	40	13.16	8.997	7.059	4.317	18	10	9	0	7.692	19.03	11	9.346	25.53	0	28.57	9.901	15.38	40	0
Std WMG-1	90	16	10	0.6	0.2	3.3	271	1.2	45	293	2276	182	6150	0.84	11.62	68	5.7	0.96	0.28	0.03	6.9	0.64	14.8	1.08
Std WMG-1	41	114	1	1	1	1170	149	770	2700	200	5900	1	15	110	7	2						1		
% Difference		86	167	58.82	105.9	124.8	107.2	90	17	10	4	50	25.39	47	20.47	60.87	200	200	200	200	52.87	200	200	200

TABLE 2, CONTINUED

Sample	ppb							ppb**			
	Re	Hg*	Ag	Au	Pt	Pd	Os	Au	Pt	Pd	Rh
01GNX 19-6-1***	1	7	111	0.9	< 2	< 10	< 1	< 1	0.2	4.9	< .05
01GNX 19-4-1	< 1	5	19	0.4	5	< 10	< 1	< 1	7.1	18.4	0.30
01GNX 19-10-1	< 1	>99999	8863	7693	6	209	< 1	7218	14.7	207.9	0.17
01GNX 19-9-1	15	26270	20563	13905	7	224	< 1	6276	2.6	192.5	0.16
01GNX 19-36-1	17	404	17391	1997	5	353	6	3074	2.9	313.4	0.12
01GNX 19-26-1	13	2901	16489	4751	71	2468	< 1	5176	143.3	2424	< .05
01GNX 19-32-1	7	615	3446	7023	24	3833	< 1	7764	92.2	3507	0.35
01GNX 19-14-1	9	411	2400	9182	6	318	< 1	3874	4.5	203.9	0.23
01GNX 19-15-1	24	1234	15013	2527	34	522	7	7564	93.8	983.4	0.12
01GNX 19-22-1	18	198	2199	1492	7	< 10	< 1	1226	6.2	19.3	0.14
01GNX 19-21-1	13	251	4849	2931	14	56	< 1	3336	11.1	53.9	0.22
01GNX 19-31-1	13	494	3388	4672	17	968	1	3608	36.3	1179	0.27
<u>Quality Control</u>											
01GNX 19-9-1	15	26270	20563	13905	7	224	< 1	6276	2.6	192.5	0.16
01GNX 19-9-1D	31	25289	20563	11466	6	231	< 1	6364	2.5	202.8	0.06
% Difference	70	4	0	19	15	3		1	4	5	91
01GNX 12-2-5	3	446	>99999	705	1842	1080	9	641	8507	1519	2.98
01GNX 12-2-5D	6	276	>99999	611	882	859	26	618	3078	1397	3.00
% Difference	67	47		14	70	23	97	4	94	8	1
GSB Std. OC-80	<1	115	53	5.5	<2	<10	<1	2	5.5	7.7	<0.1
GSB Std. OC-80	2	48	52	2.1	8	<10	<1	1	4.3	8.8	<0.1
% Difference		82	2	89				67	24	13	
Std WMG-1	20	137	2266	169	293	447	54	127	867	393.1	11.77
Std WMG-1			2700	110	731	382		110	731	382	26.0
% Difference	200	200	17	42	86	16	200	14	17	3	75

Analyses done by Acme Analytical Laboratories Ltd., Vancouver; aqua regia digestion of 1g sample (-150 mesh; steel mill; quartz wash) and ICP-MS/ES finish

\* Maximum concentration of method = 99999 ppb

\*\* Fire assay using Pb collector (15-30g sample) with ICP finish

% Difference =  $\text{Abs}((x1-x2)/((x1+x2)/2)) * 100$

\*\*\* Sample located on the 548.6m Bench ~15m north of sample 01GNX19-5-1 (Fig. 4).

wt %, weight percent; ppm, parts per million; ppb, parts per billion; D, duplicate analysis

Mineral abbreviations: Mt, magnetite; Hm, hematite; Cu, native copper; Cpy, chalcopyrite; Py, pyrite; Cc, chalcocite; Bn, bornite; Ca, carbonate (calcite/dolomite/ankerite); Qz, quartz; Chl, chlorite; Ep, epidote/zoisite/clinozoisite; Fs, alkali feldspar; Kspar, potassium feldspar; Tr-Act, tremolite-actinolite; Ap, apatite; Ser, sericite; Bi, biotite; Sp, serpentine; Cpx, clinopyroxene; Ol, olivine. Minerals in parentheses are present in minor to trace amounts.

these samples are markedly enriched in silver (2200 to >22500 ppb Ag). As with most alkaline Cu-Au porphyry deposits, molybdenum is typically low (<26 ppm Mo) along with lead (generally <30 ppm Pb) except for one anomalous sample (212 ppm Pb) which also has high molybdenum (46 ppm Mo). Locally anomalous molybdenum abundances are perhaps not unexpected since Kwong (1987) noted isolated occurrences of chalcopyrite and molybdenite just below the southern rim of the pit. The abundances of zinc are generally less than 100 ppm with one anomalous sample containing 443 ppm Zn.

It is interesting to note that the two samples from the supergene alteration zone contain extremely high levels of mercury (26 and >100 ppm Hg, Table 2). The chalcocite-bearing sample also has anomalously high Au, Ag, As and Sb, indicative of an epithermal signature. The PGE in this sample do not appear to be particularly enriched or depleted, and this may be due to the chalcocite being of hypogene origin. The sample containing native copper carries the highest mercury and has appreciable abundances of PGE (up to 15 ppb Pt and >200 ppb Pd). This raises the possibility that PGE are incorporated via solid solution in the copper alloy. However, the behaviour of PGE during supergene alteration processes is currently not well understood.

Although the aqua regia leach is only partial for iron oxides, the sample of massive magnetite is clearly a vanadiferous variety (>1000 ppm V) and contains cobalt (90 ppm Co). Trace amounts of sulphides, not detected in thin section, also appear to be present judging from the abundances of copper (968 ppm Cu) and sulphur (0.02 wt. % S). The abundances of Pt (0.2 ppb), Pd (5 ppb) and Au (<1 ppb) are near or below detection levels. As anticipated, the picrite yields the highest abundances of Ni and Cr but the lowest concentrations of base and precious metals (9 ppm Cu, 7 ppb Pt, ~18 ppb Pd and <1 ppb Au).

### ***Inter-Element Correlations***

In order to investigate inter-element variations, a correlation matrix was established for the Afton sample suite. Selected plots showing Pearson correlation coefficients are presented in Figures 9 to 11. The treatment specifically focuses on correlations among sulphide-rich samples, and excludes the picrite, magnetite vein and magnetite-carbonate-sulphide breccia (01GNX19-26-1, Appendix). Distinctions were also maintained between abundances determined by the aqua regia and fire assay methods. Some preliminary observations appear worthwhile, notwithstanding the small size of the sample population.

Moderate correlations exist between Pt, Pd and S, but not between PGE and Cu or Au, possibly due to the limited number of samples analyzed (Fig. 9). The positive correlation observed in the Cu vs Au plot parallels

observations at other deposits hosted by the Iron Mask Batholith, and has been interpreted to reflect co-precipitation of these metals during a single hydrothermal event (*e.g.* Lang and Stanley, 1995). Correlations are also evident between PGE and Fe, and the Rh vs Fe regression is particularly striking, especially in view of the semi-quantitative determination of rhodium (Fig. 10). Of further note are positive correlations (not shown) between Pt-Ti (R=0.93 using Pt determined by aqua regia) and Pt-Mo (R=0.88). The significance of these latter correlations is not presently understood.

A moderate positive correlation is apparent between Ag and Cu but not between Ag and Au, which may reflect contrasting behaviour of these metals in hydrothermal fluids. However, marked correlations are observed between Ag, Bi and U which would appear to imply that hydrothermal fluids were capable of transporting both low-field-strength and high-field-strength elements to sites of mineralization.

Scattergrams of La and Th vs Ca (Fig. 11) and La and Th vs P (not shown; R=0.73-0.79) show strong to moderate correlations. This may primarily reflect the ability of apatite to incorporate high-field-strength elements within its structure, since a positive correlation is also evident between Ca and P (R=0.68). However, an epidote-group mineral may also play a subsidiary role. The marked covariance between K and Sc (Fig. 11) may likewise reflect the presence of hydrothermal biotite in these rocks. However, despite the intimate petrographic association between potassic alteration and mineralization, no significant correlations are evident between these elements and the precious or base metals.

## **SUMMARY AND CONCLUSIONS**

A small suite of PGE-enriched, Cu-Fe-sulphide-bearing samples collected from core obtained during deep drilling beneath the Afton pit has been examined petrographically and analyzed by fire assay and aqua regia digestion ICP-ES/MS. The principal observations are as follows:

1. Mineralization is hosted by a microporphyritic diorite-monzodiorite-monzonite(-syenite) phase of the Iron Mask batholith that appears to be part of the Cherry Creek unit. The host rocks belong to the silica-saturated subclass of alkaline intrusions associated with Cu-Au porphyry deposits as defined by Lang *et al.* (1994, 1995). Samples examined in this study are microporphyritic diorite or leuco-diorite that appear to belong to the Cherry Creek unit.
2. There is good petrographic evidence for an intimate association between a potassic- or (calcic)-potassic-style of alteration and sulphide mineralization. Potassic alteration typically comprises a fine-grained assemblage of biotite-

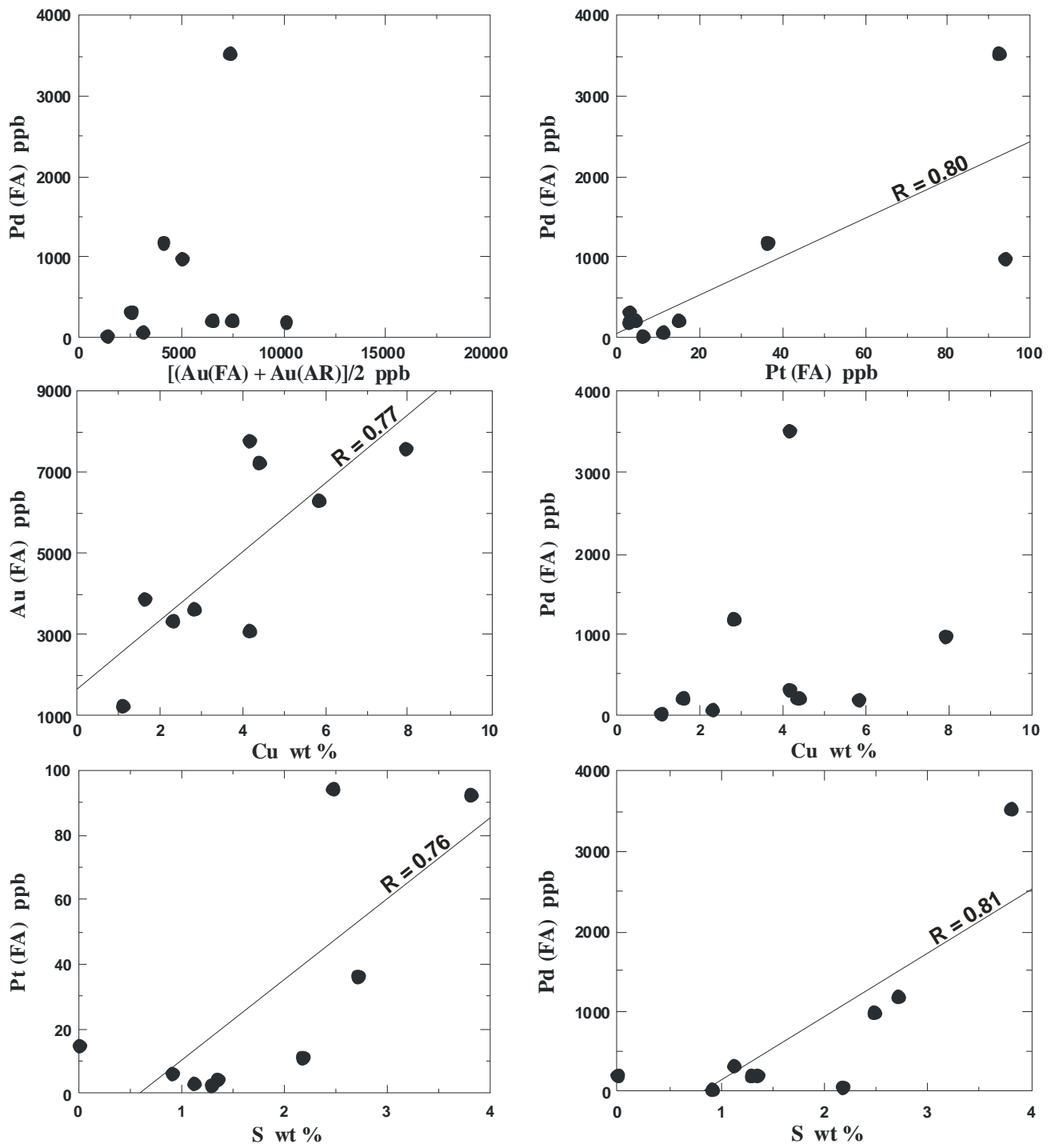


Figure 9. Scatterplots of PGE, Au, Cu and S showing Pearson correlation coefficients.

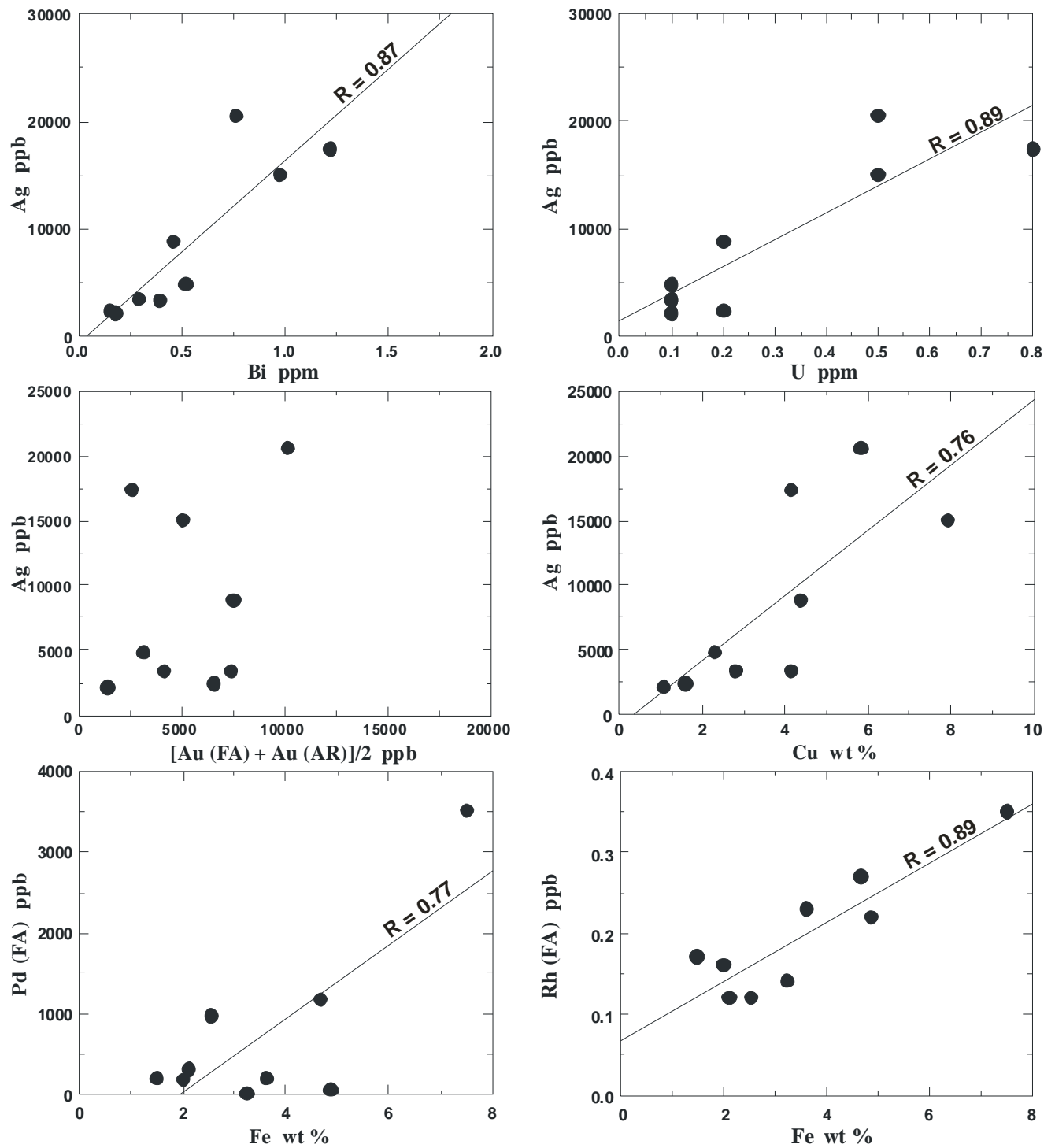


Figure 10. Scatterplots of PGE, Au, Ag, Cu, Fe, Bi and U showing Pearson correlation coefficients.

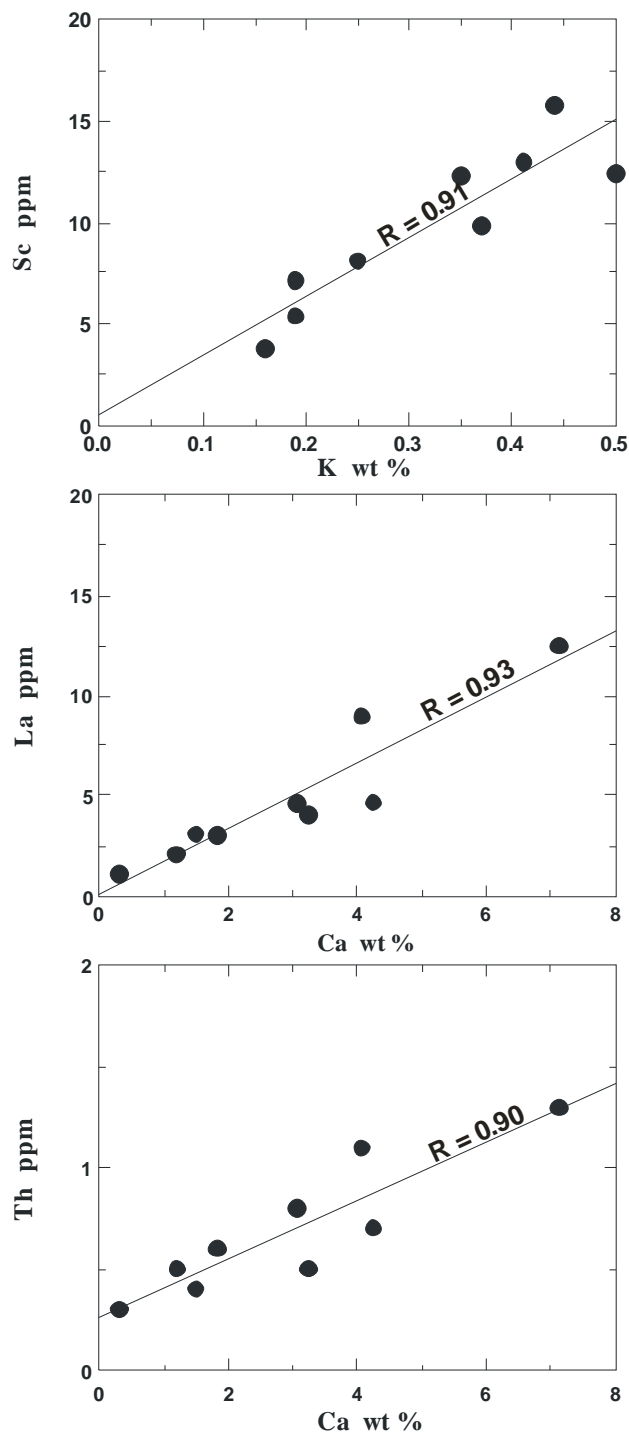


Figure 11. Scatterplots of selected non-metals showing Pearson correlation coefficients.

alkali feldspar-sericite-(minor)epidote +/- magnetite-apatite. Superimposed on this early potassic event is a locally pervasive carbonate (calcite-dolomite-ankerite) alteration and late veins of carbonate+/-quartz. Kwong (1987) notes that carbonate alteration *rarely* appears to be coincident with sulphide mineralization.

3. The principal hypogene ore minerals in the samples examined are chalcopyrite and bornite, locally altered in part to covellite, ?digenite and

secondary copper carbonates. Minor amounts of pyrite and chalcocite are present in several samples. Pyrite forms an early component of the mineralization and, where preserved, is partially replaced by Cu-Fe sulphides. Supergene minerals include chalcocite and native copper.

4. The hypogene sulphides commonly form fine to heavy disseminations and blebs which preferentially replace the fine-grained groundmass of their microporphyritic host, reflecting the efficient exploitation of grain boundaries by mineralizing hydrothermal fluids. These sulphides also occur in veins and fracture fillings.
5. The maximum abundances of PGE and associated precious metals in analyzed samples are: 3833 ppb Pd; 143 ppb Pt; 13905 ppb Au; and 20563 ppb Ag. The PGE are intimately associated with chalcopyrite and bornite, but further work is needed to characterize their exact mode of occurrence (*i.e.* solid solution in Cu-Fe sulphides or discrete platinum-group minerals). Two supergene-altered samples carrying native copper and (?hypogene) chalcocite show no obvious depletion or enrichment of PGE.
6. Pd abundances are highly anomalous in 8 out of 10 samples with greater than 1 wt. % Cu, and four samples have 0.98 to 3.8 g/t Pd.
7. Correlations between PGE and elements that may serve as potential geochemical "pathfinders" are generally poor. A moderate positive correlation is statistically evident between PGE and sulphur, but not between PGE and Cu or Au in this small sample suite. The significance of a relatively good covariance between Rh and Fe is not currently understood.
8. The aqua regia digestion method for PGE appears to provide a reliable indication of Pd abundances when compared to fire assay results. However, the former method systematically underestimates Pt abundances in these Cu-Fe-sulphide-bearing samples.

This study is part of an ongoing investigation of alkaline Cu-Au porphyry deposits in British Columbia which is attempting to provide baseline geochemical and mineralogical data for the PGE in these alkaline-associated hydrothermal systems.

## ACKNOWLEDGMENTS

The staff of DRC Resources Corporation are thanked for permission to sample core and for providing geological information on the Afton deposit, in particular John Kruzick, John Ball and Marek Mroczek; and Chris Sebert kindly provided a geological tour of the pit. Consulting geologist J. J. McDougall is thanked for lively

discussions concerning the Afton deposit; and Mike Cathro shared his knowledge of the regional geology and organized a fieldtrip to the Iron Mask Batholith for participants of the 2003 GAC-MAC Annual General Meeting held last May in Vancouver. Jack Ebbels and Ron Smyth first suggested the Afton study, Brian Grant provided logistical support, Mike Fournier drafted Figure 3, Dave Lefebure kindly provided editorial comments, and Garry Payie prepared the final manuscript for publication.

## REFERENCES

- Barr, D. A., Fox, P. E., Northcote, K. E. and Preto, V. A. (1976): The alkaline suite porphyry deposits - a summary; in *Porphyry Deposits of the Canadian Cordillera*, Sutherland Brown, A., Editor, *Canadian Institute of Mining and Metallurgy*, Special Volume 15, pages 359-367.
- Carr, J. M. (1956): Copper deposits associated with the eastern part of the Iron Mask Batholith near Kamloops; *B. C. Minister of Mines Annual Report*, 1956, pages 47-69.
- Carr, J. M. and Reed, A. J. (1976): Afton: a supergene copper deposit; in *Porphyry Deposits of the Canadian Cordillera*, A. Sutherland Brown (Editor), *Canadian Institute of Mining and Metallurgy*, Special Volume 15, pages 376-387.
- Cockfield, W. E. (1948): Geology and mineral deposits of Nicola map area, British Columbia; *Geological Survey of Canada*, Memoir 249, 164 pages.
- Dunn, C. E., Hall, G. E. M. and Nixon, G. (2001): Orientation study of surface geochemical methods to assist in the exploration for platinum-group metals in the Whiterocks Mountain alkalic complex, near Kelowna, British Columbia (82L/4); in *Geological Fieldwork 2000*, B. C. Ministry of Energy and Mines, Paper 2001-1, pages 223-230.
- Ewing, T. E. (1981): Regional stratigraphy and structural setting of the Kamloops Group, south-central British Columbia; *Canadian Journal of Earth Sciences*, Volume 18, pages 1464-1477.
- Hoiles, H. H. K. (1978): Nature and genesis of the Afton copper deposit, Kamloops, British Columbia; Unpublished M.Sc. Thesis, *The University of Alberta*, Edmonton, Alberta, 186 pages.
- Hulbert, L. J. (2001): Digital map and database of mafic-ultramafic hosted Ni, Ni-Cu, Cr +/- PGE occurrences and mafic-ultramafic bodies in British Columbia; *B. C. Ministry of Energy and Mines*, Geoscience Map 2001-2.
- Irvine, T. N. and Baragar, W. R. A. (1971): A guide to the chemical classification of the common volcanic rocks; *Canadian Journal of Earth Sciences*, Volume 8, pages 523-548.
- Kwong, Y. T. J. (1982): A new look at the Afton copper mine in the light of mineral distributions, host rock geochemistry and irreversible mineral-solution interactions; Unpublished Ph.D. thesis, *The University of British Columbia*, 121 pages.
- Kwong, Y. T. J. (1987): Evolution of the Iron Mask Batholith and its associated copper mineralization; *B. C. Ministry of Energy, Mines and Petroleum Resources*, Bulletin 77, 55 pages.
- Kwong, Y. T. J., Greenwood, H. J. and Brown, T. H. (1982): A thermodynamic approach to the understanding of the supergene alteration at the Afton copper mine, south-central British Columbia; *Canadian Journal of Earth Sciences*, Volume 19, pages 2378-2386.
- Lang, J. R. and Stanley, C. R. (1995): Contrasting styles of alkalic porphyry copper-gold deposits in the northern Iron Mask Batholith, Kamloops, British Columbia; in *Porphyry deposits of the Northwestern Cordillera of North America*, T. G. Schroeter (Editor), *Canadian Institute of Mining, Metallurgy and Petroleum*, Special Volume 46, pages.
- Lang, J. R., Stanley, C. R. and Thompson, J. F. H. (1994): Porphyry copper deposits related to alkalic igneous rocks in the Triassic-Jurassic arc terranes of British Columbia; in *Footprints Along the Cordillera*, J. G. Bolm and Pierce, F. W. (Editors), *Arizona Geological Society Digest*, Volume 20, pages 219-236.
- Lang, J. R., Lueck, B., Mortensen, J. K., Russell, J. K., Stanley, C. R., and Thompson, J. F. H. (1995): Triassic-Jurassic silica-undersaturated and silica-saturated intrusions in the Cordillera of British Columbia: implications for arc magmatism; *Geology*, Volume 23, pages 451-454.
- LeMaitre, R. W. (Editor) (1989): A classification of igneous rocks and glossary of terms, *Blackwell Scientific Publications*, Oxford, 193 pages.
- LeMaitre, R. W. (1976): Some problems of the projection of chemical data into mineralogical classifications; *Contributions to Mineralogy and Petrology*, Volume 56, pages 181-189.
- Mortensen, J. K., Ghosh, D. K. and Ferri, F. (1995): U-Pb geochronology of intrusive rocks associated with copper-gold porphyry deposits in the Canadian Cordillera; in *Porphyry Deposits of the northwestern Cordillera of North America*, T. G. Schroeter (Editor), *Canadian Institute of Mining, Metallurgy and Petroleum*, Special Volume 46, pages 142-158.
- Nixon, G. T. (2001): Alkaline-hosted Cu-PGE mineralization in British Columbia: the Whiterocks Mountain plutonic complex, south-central B. C.; *B. C. Ministry of Energy and Mines*, Open File 2001-14.
- Nixon, G. T. (2002): Cu-PGE mineralization in alkaline plutonic complexes; *B. C. Ministry of Energy and Mines*, Geofile 2002-2.
- Nixon, G. T. (2003): Geological setting of the Lorraine Cu-Au porphyry deposit, Duckling Creek Syenite Complex, north-central British Columbia; *B. C. Ministry of Energy and Mines*, Geofile 2003-5.
- Nixon, G. T. and Archibald, D. A. (2002): Age of platinum-group-element mineralization in the Sappho alkaline complex, south-central British Columbia; in *Geological Fieldwork 2001*, B. C. Ministry of Energy and Mines, Paper 2002-1, pages 171-176.
- Nixon, G. T. and Carbno, B. (2001): Whiterocks Mountain alkaline complex, south-central British Columbia: geology and platinum-group-element mineralization; in *Geological Fieldwork 2000*, B. C. Ministry of Energy and Mines, Paper 2001-1, pages 191-222.
- Nixon, G. T. and Peatfield, G. R. (2003): Geological setting of the Lorraine Cu-Au porphyry deposit, Duckling Creek Syenite Complex, north-central British Columbia; *B. C. Ministry of Energy and Mines*, Open File 2003-4, 24 pages.

- Northcote, K. E. (1974): Geology of the northwest half of the Iron Mask Batholith; in Geological Fieldwork 1974, B. C. Ministry of Energy, Mines and Petroleum Resources, Paper 1975-1, pages 22-26.
- Northcote, K. E. (1976): Geology of the southeast half of the Iron Mask Batholith; in Geological Fieldwork 1976, B. C. Ministry of Energy, Mines and Petroleum Resources, Paper 1977-1, pages 41-46.
- Northcote, K. E. (1977): Preliminary Map No. 26 (Iron Mask Batholith) and accompanying notes; B. C. Ministry of Energy, Mines and Petroleum Resources, 8 pages.
- Palfy, J., Smith, P. L. and Mortensen, J. K. (2000): A U-Pb and <sup>40</sup>Ar-<sup>39</sup>Ar time scale for the Jurassic; *Canadian Journal of Earth Sciences*, Volume 37, pages 923-944.
- Preto, V. A. (1967): Geology of the eastern part of the Iron Mask Batholith; B. C. Minister of Mines Annual Report, 1967, pages 137-147.
- Preto, V. A. (1972): Report on Afton, Pothook; B. C. Ministry of Energy, Mines and Petroleum Resources, Geology, Exploration and Mining 1972, pages 209-220.
- Ross, K. V., Godwin, C. I., Bond, L. and Dawson, K. M. (1995): Geology, alteration and mineralization in the Ajax East and Ajax West deposits, southern Iron Mask Batholith, Kamloops, British Columbia; in Porphyry Deposits of the northwestern Cordillera of North America, T. G. Schroeter (Editor), *Canadian Institute of Mining, Metallurgy and Petroleum*, Special Volume 46, pages 565-580.
- Snyder, L. D. (1994): Petrological studies within the Iron Mask Batholith, south-central British Columbia; Unpublished M.Sc. thesis, *The University of British Columbia*, Vancouver, British Columbia, 192 pages.
- Snyder, L. D. and Russell, J. K. (1993): Field constraints on diverse igneous processes in the Iron Mask Batholith (92L/9); in Geological Fieldwork 1992, B. C. Ministry of Energy, Mines and Petroleum Resources, Paper 1993-1, pages 281-286.
- Snyder, L. D. and Russell, J. K. (1995): Petrogenetic relationships and assimilation processes in the alkalic Iron Mask batholith, south-central British Columbia; ; in Porphyry Deposits of the northwestern Cordillera of North America, T. G. Schroeter (Editor), *Canadian Institute of Mining, Metallurgy and Petroleum*, Special Volume 46, pages 593-608.

## APPENDIX: PETROGRAPHIC DESCRIPTIONS OF MINERALIZED SAMPLES

### Sample: 01GNX19-6-1

**Location:** East wall of Afton pit (548.6 m Bench)  
Easting 676031 Northing 5615102  
(UTM Zone 10 NAD 83)

**Rock Type:** Magnetite vein cutting microdiorite

**Ore Minerals:** Magnetite

**Alteration:** Epidote-rich envelope with subordinate chlorite

**Description:** Magnetite is semi-massive or forms granular compact grains rarely showing faceted boundaries against carbonate and silicates; minor patchy alteration of magnetite to hematite is observed in reflected light. Minor amounts of very pale green chlorite and granular, weakly pleochroic to colourless epidote are intergrown with the magnetite. A brownish nearly opaque mixture of goethite/limonite occurs locally and trace amounts of colourless subhedral apatite. No sulfides were observed despite careful examination in reflected light. The rock is cut by thin veinlets of colourless carbonate + minor quartz + trace hematite/limonite.

**Comments:** Sample was collected from the centre of the vein.

### Sample: 01GNX19-4-1

**Location:** DDH 2K01 Box 25 23.35 m  
Easting 675610 Northing 5614869

**Rock Type:** Porphyritic olivine-clinopyroxene basalt

**Ore Minerals:** Pyrite (trace)

**Alteration:** Tremolite-actinolite and secondary Fe oxides

**Description:** Clinopyroxene occurs as large (<3 mm), virtually unaltered, pale brown (oxidized) to very pale green phenocrysts with mostly euhedral to subhedral outlines. A few crystals are resorbed and some have devitrified and altered glass inclusions. Some phenocrysts preserve core to rim zoning, and several grains are partially altered to tremolite-actinolite. The texture is hiatal with a few euhedral microphenocrysts in the groundmass. Subhedral to rounded phenocrysts of olivine are completely replaced by fibrous tremolite-actinolite and fine-grained Fe oxides +/- minor serpentine. Some olivines form glomeroporphyritic clots. The groundmass is formed by fine-grained tremolite-actinolite, feldspar, pyroxene, and opaques and clay minerals (on feldspar sites). The only sulfide present is disseminated subhedral pyrite (<1%). A few irregular veinlets of altered feldspar and carbonate cut the rock.

**Comments:** This clinopyroxene-olivine-phyric basalt appears to represent a fault sliver of picrite wallrock. Note the presence of pyrite, lack of Cu-Fe sulfides, and alteration assemblages equivalent to the uppermost greenschist facies.

**Sample: 01GNX19-10-1**

*Location:* DDH 2K05 Box 37 224.2 m  
Easting 675581 Northing 5614871

*Rock Type:* Quartz-bearing microporphyritic diorite/leucodiorite

*Ore Minerals:* Native Cu

*Alteration:* Argillic, weak sericitic

*Description:* Plagioclase occurs as pale brownish euhedral to anhedral laths and subequant crystals (<1.5 mm) with a subparallel magmatic foliation. Most grains are partially altered to clay minerals and minor sericite. Interstitial anhedral quartz grains (<0.8 mm) are locally intergrown with opaque material and it is not clear whether they are magmatic or hydrothermal in origin. Microcrystalline opaques comprise goethite/pitch limonite with interspersed very fine-grained hematite. A few large (1-2 mm) irregular grains of native copper are associated with the fine-grained opaques. Granular hematite +/- quartz is also found in anastomosing narrow veinlets cutting the rock.

*Comments:* The presence of native Cu indicates the presence of the supergene zone at this depth.

**Sample: 01GNX19-9-1**

*Location:* DDH 2K05 Box 37 225.2m  
Easting 675581 Northing 5614871

*Rock Type:* Carbonatized diorite/leucodiorite

*Ore Minerals:* Chalcocite

*Alteration:* Pervasively carbonatized

*Description:* Pale brown, subhedral relict plagioclase crystals (<1.5 mm) with inequigranular textures have been extensively replaced by clay minerals, fine-grained granular carbonate and sericite flecks; some grains preserve albite twinning; colourless calcite occurs in disseminations and veinlets accompanied by minor quartz and sulfide; no relict mafic minerals can be identified; an anastomosing vein network controls the distribution of chalcocite which is the only sulfide mineral identified.

*Comments:* Note the lack of pyrite.

**Sample: 01GNX19-36-1**

*Location:* DDH 2K08 Box 19 142.5 m  
Easting 675581 Northing 5614871

*Rock Type:* Carbonatized inequigranular leucodiorite(?)

*Ore Minerals:* Bornite (-chalcopyrite-covellite-?digenite)

*Alteration:* Intensely carbonatized with moderate sericite development

*Description:* Plagioclase occurs as pale brown subhedral to anhedral grains (<1 mm) which locally preserve lamellar twinning, and some crystals have well-developed subgrain mosaic boundaries. The feldspars are extensively altered to microcrystalline granular carbonate, sericite and minor clay minerals. No pseudomorphs after mafic minerals have been identified. The dominant sulfide mineral is bornite which encloses trace amounts of tiny (<20 µm) chalcopyrite blebs and is partially altered to covellite and ?digenite. Rare, minute (<20 µm) grains of

brown pleochroic biotite are found as inclusions in the bornite. The sulfides are both disseminated and fracture-controlled. Trace quantities of magnetite and hematite occur as tiny grains dispersed among the silicates. The rock is cut by numerous irregular veinlets of carbonate + quartz + minor apatite + sulfides + trace amounts of chlorite and limonite.

*Comments:* Textures are similar to sample 01GNX19-9-1 but the rock is more pervasively altered. The distribution and texture of the sulfides, and the presence of tiny inclusions of biotite, are features consistent with a hydrothermal origin.

**Sample: 01GNX19-26-1**

*Location:* DDH 01-24 Box 62 349.8 m  
Easting 675429 Northing 5614712

*Rock Type:* Sulfide bleb in magnetite-carbonate vein/breccia/replacement in diorite

*Ore Minerals:* Magnetite-chalcopyrite(-pyrite)

*Alteration:* Magnetite-carbonate-apatite

*Description:* Magnetite occurs as non-faceted, granular crystals crosscut by irregular carbonate-filled microfractures and is locally intergrown with, or marginal to, the sulfides. Colourless euhedral to subhedral crystals of apatite (<0.8 mm) commonly contain tiny opaque inclusions. Apatite may form monomineralic aggregates or localized integrowths with magnetite, carbonate and sulfide. Anhedral crystals (<1.2 mm) of patchy zoned alkali feldspar are intergrown with magnetite and sulfide, and partially altered to carbonate, sericite and clay minerals. One large sulfide-rich bleb, several centimetres across, was examined in reflected light. Massive to disseminated chalcopyrite, the dominant sulfide, is intensely fractured and veined by carbonate, and contains minor inclusions of subhedral to anhedral and resorbed pyrite crystals. No secondary Cu sulfides have been identified. The rock is cut by narrow irregular veinlets of carbonate and quartz.

*Comments:* Note the presence of chalcopyrite and pyrite. Textural relationships indicate that pyrite is early and partially resorbed by the Cu-rich hydrothermal fluids which precipitated chalcopyrite.

**Sample: 01GNX19-32-1**

*Location:* DDH 01-27 Box 44 234.3 m  
Easting 675571 Northing 5614876

*Rock Type:* Potassic-altered microporphyritic diorite

*Ore Minerals:* Chalcopyrite

*Alteration:* Carbonate-sericite-biotite(-chlorite-potassium feldspar)

*Description:* Plagioclase occurs as euhedral to subhedral laths and subequant crystals (<1.5 mm) set in a fine-grained, altered feldspathic groundmass. Many crystals preserve lamellar twinning and display a subparallel magmatic flow foliation. The feldspars are extensively replaced by microcrystalline carbonate + sericite + reddish brown pleochroic biotite flakes. This secondary biotite is intergrown with sulfides and locally

accompanied by minor potassium feldspar and pale green, weakly pleochroic chlorite (mostly pseudomorphous after biotite). The only sulfide identified is very fine to coarsely disseminated chalcopyrite (5-10 %). The rock also contains minor disseminated magnetite (~1 vol. %) locally altered to hematite +/- ilmenite. Colourless carbonate veinlets cut the potassic alteration and thus are very late.

*Comments:* The presence of secondary biotite intergrown with chalcopyrite clearly points to a potassic style of hydrothermal alteration accompanying introduction of the sulfides.

**Sample: 01GNX19-14-1**

*Location:* DDH 01-27 Box 45 241.8 m  
Easting 675571 Northing 5614876

*Rock Type:* Carbonatized and sericitized microporphyritic diorite

*Ore Minerals:* Chalcopyrite

*Alteration:* Carbonate-sericite

*Description:* Plagioclase occurs as very pale brownish euhedral to anhedral, mostly subequant crystals (<1 mm) set in a fine-grained feldspathic groundmass. Lamellar twinning is well preserved in some grains, and no obvious primary flow fabric is evident. Feldspar sites are partially altered to microcrystalline carbonate + sericite + minor clay minerals. Localized intergrowths of carbonate + chlorite + opaque minerals may represent pseudomorphs after a primary mafic mineral (hornblende?). Minor patches of euhedral to subhedral colourless apatite, commonly with oriented inclusions of opaque material, appear to be secondary in origin. The sulfides (~5 %) occur as disseminations and veinlets of finely crystalline chalcopyrite. The rock contains minor chlorite but appears to lack biotite.

*Comments:* Textures indicate a hydrothermal origin for the sulfides.

**Sample: 01GNX19-15-1**

*Location:* DDH 01-31 Box 6 33.8 m  
Easting 675864 Northing 5614940

*Rock Type:* Potassic-altered inequigranular microdiorite

*Ore Minerals:* Bornite

*Alteration:* Biotite-sericite(-carbonate-clay-epidote-potassium feldspar)

*Description:* Euhedral to anhedral laths and subequant crystals (<1.5 mm) of pale brownish plagioclase are partially altered to microcrystalline carbonate + sericite + biotite + opaques +/- minor epidote and clay minerals. Some grains preserve albite twinning. Localized carbonate + opaques +/- epidote +/- potassium feldspar intergrowths may represent pseudomorphs of mafic minerals. Finely disseminated and fracture controlled bornite is very fresh and lacks alteration to secondary copper sulfides. Chalcopyrite appears to be absent. The sulfides are clearly associated with secondary, reddish brown pleochroic biotite and minor very pale

green to colourless epidote. Disseminated Fe-Ti oxide grains are locally mottled and may be enclosed by bornite.

*Comments:* The textural features of sulfides and their association with secondary biotite +/- minor epidote indicate a hydrothermal origin for the mineralization.

**Sample: 01GNX19-22-1**

*Location:* DDH 01-37 Box 73 411.4 m  
Easting 675166 Northing 5614785

*Rock Type:* Microporphyritic diorite

*Ore Minerals:* Chalcopyrite(-chalcocite)

*Alteration:* Carbonate-sericite(-biotite-feldspar)

*Description:* Plagioclase forms euhedral to anhedral, subequant crystals (<1 mm) set in an altered feldspathic groundmass. Lamellar twinning is preserved locally and no magmatic foliation is evident. Feldspars are partially altered to very fine grained sericite + colourless carbonate + minor clay minerals. Disseminated, patchy and locally fracture-controlled sulfides are associated with minor albitic feldspar and trace amounts of reddish brown, altered biotite and limonite. The rock is cut by late veins of colourless carbonate.

*Comments:* This non-polished thin section prevented identification of sulfides in reflected light. From the hand sample and cut block, the sulfides appear to be predominantly chalcopyrite, possibly accompanied by minor chalcocite.

**Sample: 01GNX19-21-1**

*Location:* DDH 01-37 Box 73 413.5 m  
Easting 675166 Northing 5614785

*Rock Type:* Potassic-altered inequigranular to microporphyritic leucodiorite

*Ore Minerals:* Chalcopyrite(-pyrite)

*Alteration:* Biotite-sericite(-carbonate)

*Description:* Plagioclase forms pale brownish, euhedral to anhedral subequant crystals (<1 mm) partially altered to fine-grained sericite + biotite + minor colourless carbonate and clay minerals. Minor anhedral potassium feldspar in the groundmass may be primary. Disseminated biotite displays reddish brown pleochroism and is locally altered to green biotite/chlorite. Sulfides are primarily associated with biotite and minor quartz, albitic feldspar and euhedral to subhedral colourless apatite prisms containing oriented opaque inclusions. Minor quartz grains commonly exhibit sweeping extinction and subgrain boundaries. Sulfides, principally chalcopyrite, have a patchy distribution and in part are controlled by anastomosing microfractures. The chalcopyrite lacks any sign of alteration to secondary copper sulfides. Subhedral to fractured and broken and partially resorbed crystals of pyrite form a minor proportion of the sulfide and appear to have formed earlier than the chalcopyrite. Rounded "inclusions" of chalcopyrite in pyrite are interpreted as an artifact of the plane of section and represent re-entrants of chalcopyrite formed during dissolution of the pyrite.

*Comments:* The sulfides in this rock were deposited during alteration by potassium-rich hydrothermal fluids. The rock contains both pyrite and chalcopyrite. The pyrite

formed early and has been partially replaced by chalcopyrite.

**Sample: 01GNX19-31-1**

*Location:* DDH 01-37 Box 74 419.5 m  
Easting 675166 Northing 5614785

*Rock Type:* Potassic-altered microporphyritic diorite/monzonite

*Ore Minerals:* Chalcopyrite

*Alteration:* Biotite-sericite(-potassium feldspar?)

*Description:* Plagioclase in this rock forms pale brownish, subhedral to anhedral subequant crystals (<1.6 mm) set in a finer grained feldspathic groundmass. Lamellar twinning is locally well preserved and most grains are partially altered to microcrystalline sericite + biotite + minor clay minerals. Potassium feldspar in this rock occurs interstitial to the plagioclase and it is difficult to discern if it is primary or introduced. Minor pale green chlorite and colourless carbonate form localized granular patches. Colourless monomineralic apatite concentrations are present locally. Sulfides occur in veinlets and as disseminations, and are associated with minor albitic feldspar, chlorite and biotite. Late veinlets of calcite cut the rock.

*Comments:* This non-polished thin section prevented identification of sulfides in reflected light. From the hand sample and cut block, the sulfides appear to be predominantly chalcopyrite.

**ADDITIONAL SAMPLES:**

**Sample: 01GNX19-30-1/2**

*Location:* DDH 01-37 Box 75 419.9 m (0.4 m below 01GNX19-31-1)  
Easting 675166 Northing 5614785

*Rock Type:* Potassic-altered inequigranular to microporphyritic diorite

*Ore Minerals:* Chalcopyrite(-pyrite)

*Alteration:* Biotite-sericite-alkali feldspar-carbonate

*Description:* Very pale brown euhedral to subhedral plagioclase (<1.2 mm) is lightly dusted by sericite and clay minerals, and is locally replaced by fine-grained intergrowths of pale brown, pleochroic biotite. The larger plagioclase crystals may preserve albite twinning. Ovoid to rectangular areas of fine-grained intergrowths of chlorite+opaque oxides/leucoxene+clay-sericite-altered feldspar may represent pseudomorphs of a primary mafic mineral (?hornblende). The sulfides occur as fine disseminations and blebs, and in veinlets, and show curvilinear to finely crenulated contacts with the silicates. Chalcopyrite (~12 vol. %) contains subhedral to strongly resorbed crystals of pyrite (1-2 vol. %) and is intimately associated with secondary alkali feldspar and biotite. The rock is cut by a few veins of potassium feldspar and chlorite, and later veinlets of colourless carbonate.

*Comments:* The copper mineralization is demonstrably associated with alkali-rich hydrothermal fluids and postdates the formation of pyrite in this rock.

**Sample: 01GNX19-11-1**

*Location:* DDH 2K02 Box 59 374.8 m  
Easting 675610 Northing 5614869

*Rock Type:* Microporphyritic diorite

*Ore Minerals:* Bornite-chalcopyrite

*Alteration:* Incipient clay-sericite-chlorite-carbonate

*Description:* Pale brownish plagioclase (<2 mm) occurs as subhedral phenocrysts which grade serially towards the fine-grained feldspathic groundmass. Phenocryst margins appear weakly corroded; alternatively, this finely crenulated margin may reflect the final stages of growth into the groundmass. The larger feldspars locally preserve lamellar twinning and are lightly dusted by minute sericite flakes, clay minerals and rare carbonate. Groundmass feldspars show similar alteration and are locally intergrown with colourless euhedral to subhedral apatite (<0.2 mm), anhedral chlorite (<0.5 mm), which may be partly pseudomorphous after biotite, and minor leucoxene and ?secondary anhedral quartz (<1 vol. %). Disseminated sulfides are preferentially found in the groundmass and locally appear controlled by phenocryst margins. Bornite (~5 vol. %), which shows incipient alteration to chalcocite and covellite, is intergrown with minor chalcopyrite (~2 %). Sulfide-groundmass contacts are commonly highly irregular and appear corrosive. The sulfides contain inclusions of euhedral quartz and rare minute flakes of pale brown biotite. The rock is cut by narrow veinlets of carbonate +/- quartz.

*Comments:* The distribution and textures of the sulfides bear some resemblance to those of orthomagmatic sulfides. However, the very finely crenulated sulfide-silicate contacts, and the intimate association of sulfides with quartz and biotite, indicate a hydrothermal origin. The absence of pyrite is noteworthy.

